CINtec® p16^{INK4a} Staining Atlas

mtm

Rating

Rating

“<u>Positive</u>”

The rating “positive” will be assigned if the p16^{INK4a}-stained slide shows a continuous staining of cells of the basal and parabasal cell layers of the squamous cervical epithelium, with or without staining of cells of superficial cell layers (“diffuse staining pattern”).

Diffuse Staining Pattern:

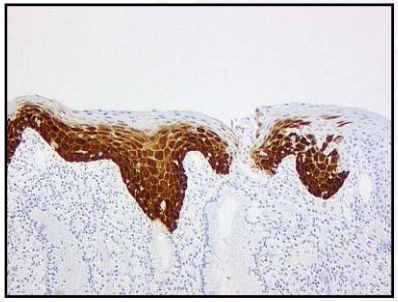

CIN2

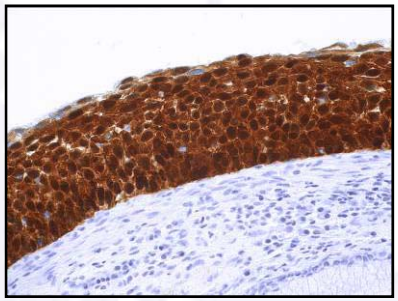

CIN3

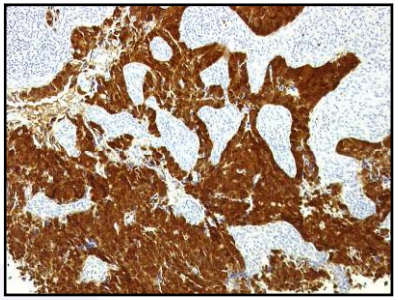

Invasive carcinoma

Rating

“Negative”

The rating “negative” will be assigned if the p16^{INK4a}-stained slide shows either a negative staining reaction in the squamous epithelium (“negative staining pattern”), or a staining of isolated cells or small cell clusters; i.e., a non-continuous staining, particularly not of the basal and parabasal cells (“focal staining pattern”).

Negative Staining Pattern:

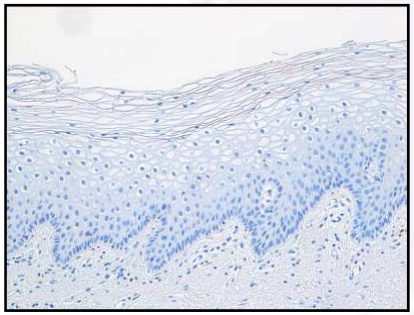

Normal squamous epithelium

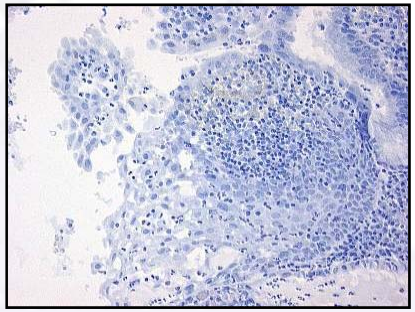

Squamous meta-plasia, immature

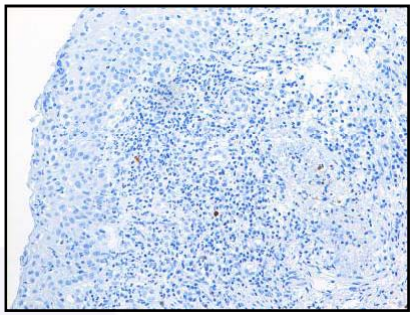

Cervicitis

Rating

“Negative”

The rating “negative” will be assigned if the p16^{INK4a}-stained slide shows either a negative staining reaction in the squamous epithelium (“negative staining pattern”), or a staining of isolated cells or small cell clusters; i.e., a non-continuous staining, particularly not of the basal and parabasal cells (“focal staining pattern”).

Focal Staining Pattern:

Squamous metaplasia, mature

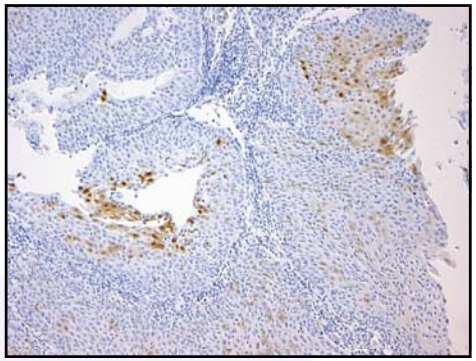

Squamous metaplasia, mature

CINtec® p16^{INK4a} Histology

- Strong diffuse p16^{INK4a}-specific immuno-reactivity in dysplastic cervical lesions

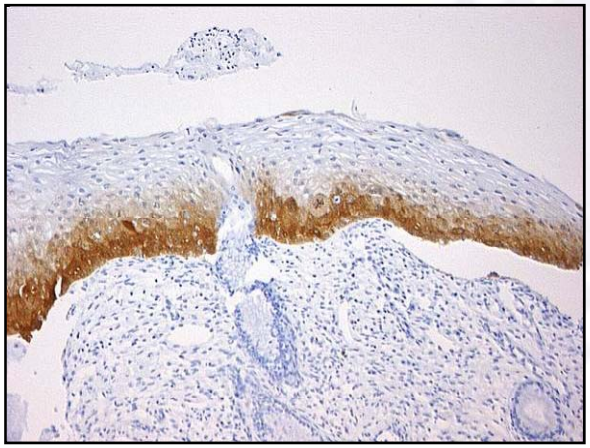

CIN1

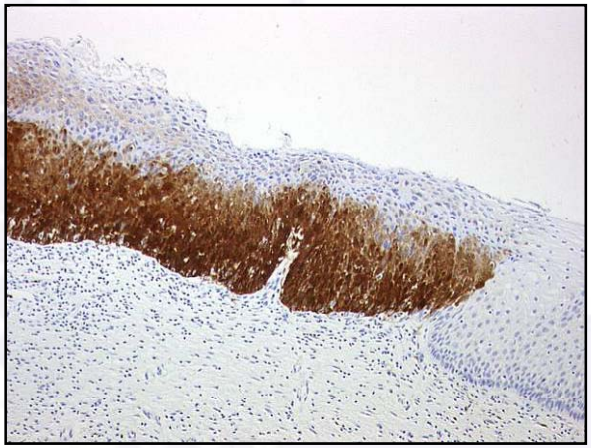

CIN2

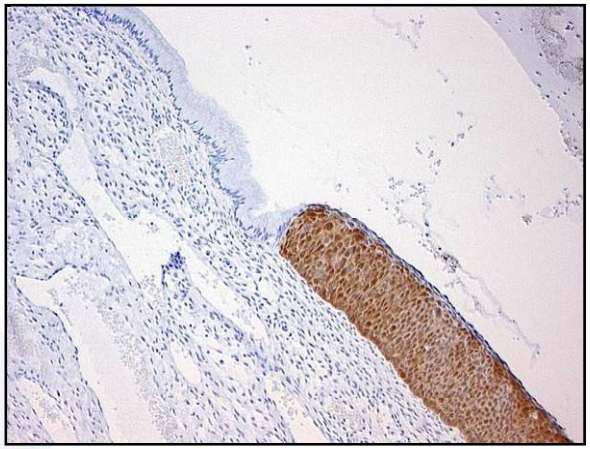

CIN3

CINtec® p16^{INK4a} Histology

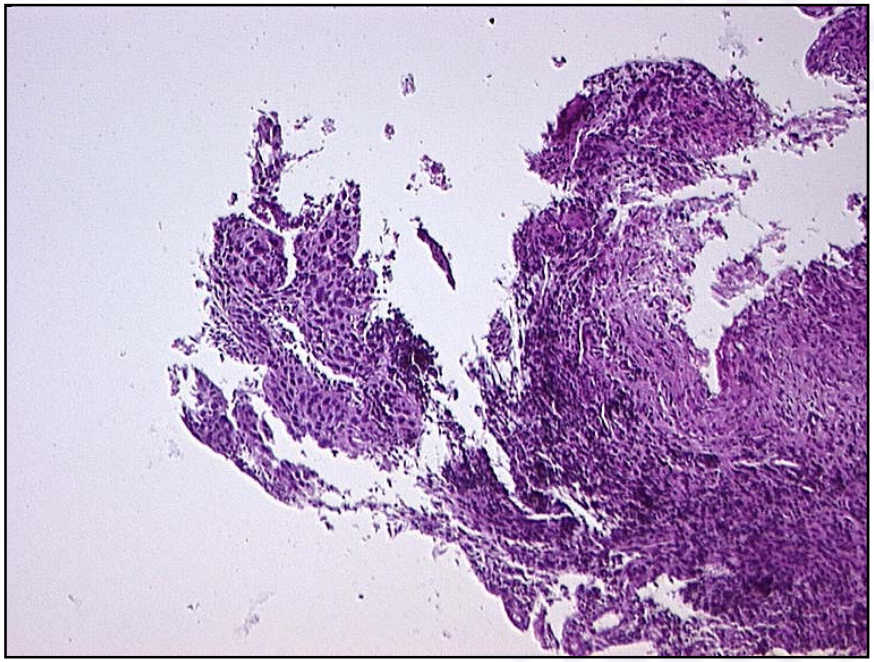

Conventional H&E

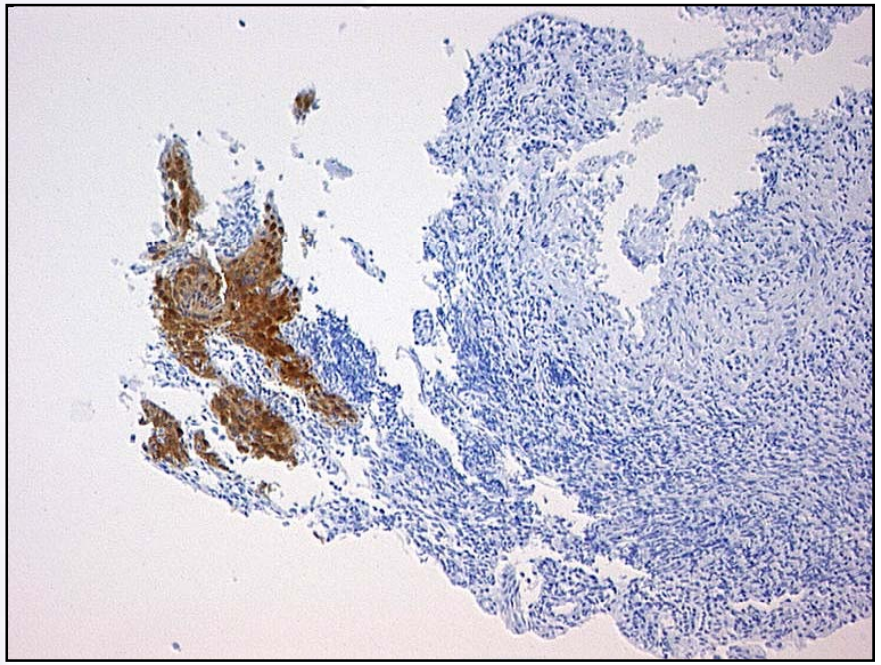

CINtec® p16^{INK4a}

CIN3 – severe dysplasia

CINtec® p16^{INK4a} Histology

- Potential increased reproducibility in diagnosing cervical lesions by p16^{INK4a} IHC

Consensus diagnosis:

no lesion

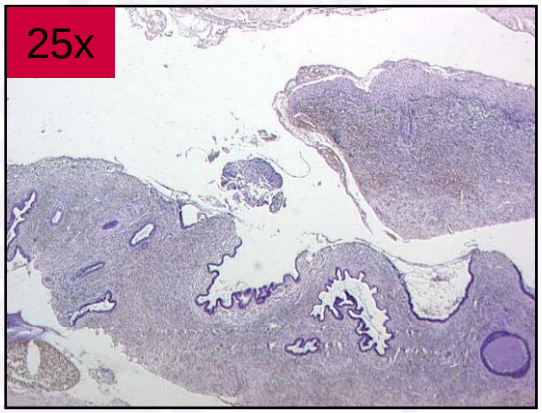

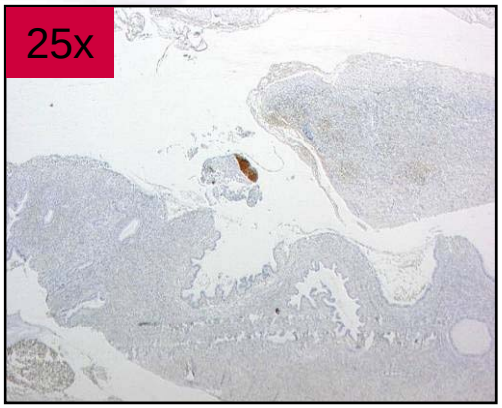

High-grade lesion detected by p16^{INK4a} IHC

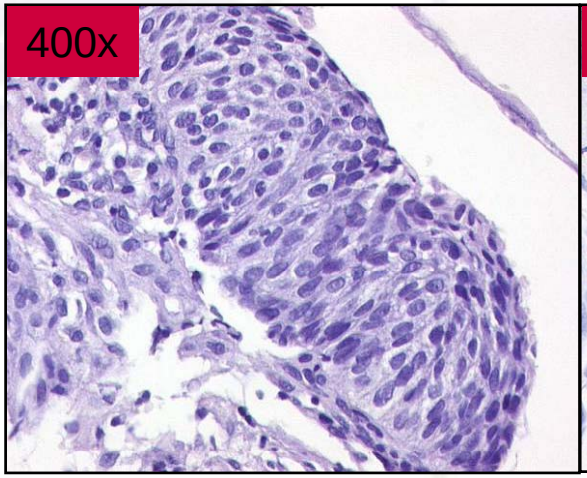

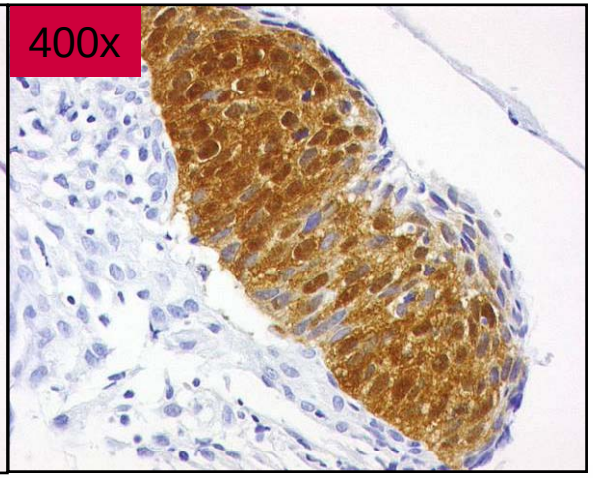

Dysplasia, caused by HR-HPV

p16^{INK4a} Immunostain: diffuse distribution of (+) cells in immature layers

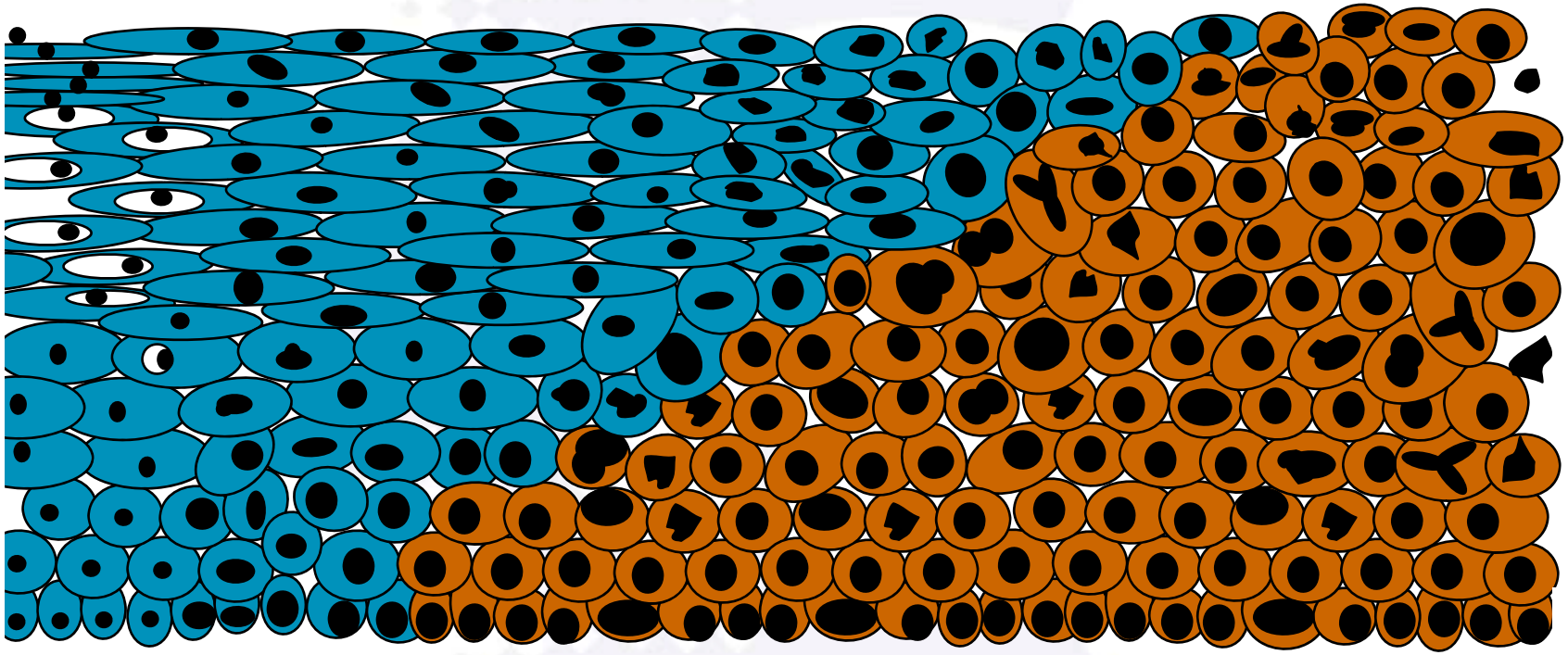

Stained cells may reach the surface of the epithelium

Invasive squamous carcinoma

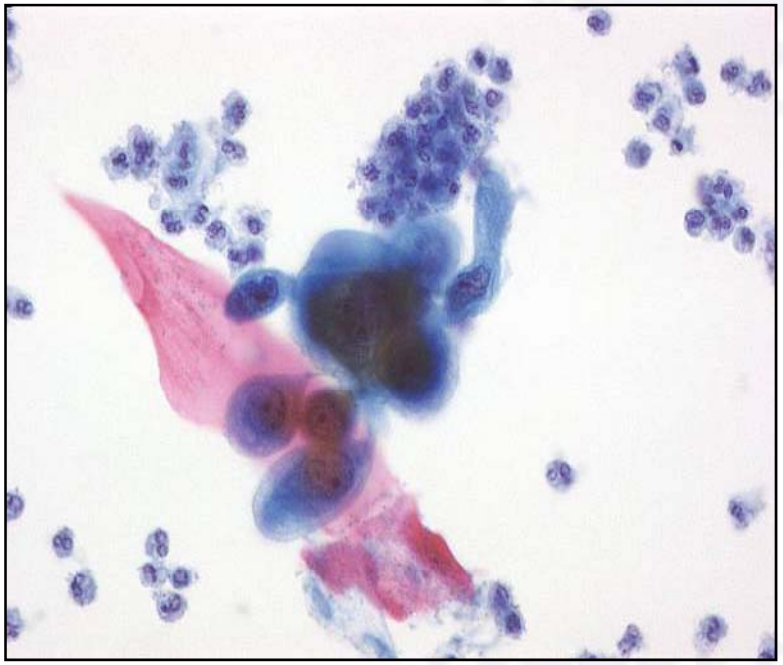

Fig. 2a: Tumor cells with marked variation of nuclear size and shape. Marked inflammatory background.

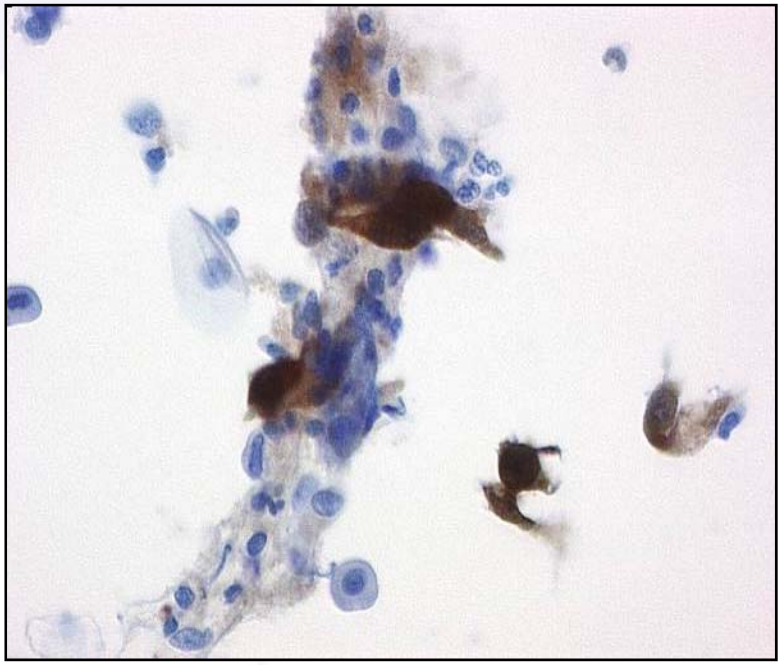

Fig. 2b: Strong positivity for $p16^{INK4a}$ in cytoplasm and nuclei.

Invasive squamous carcinoma

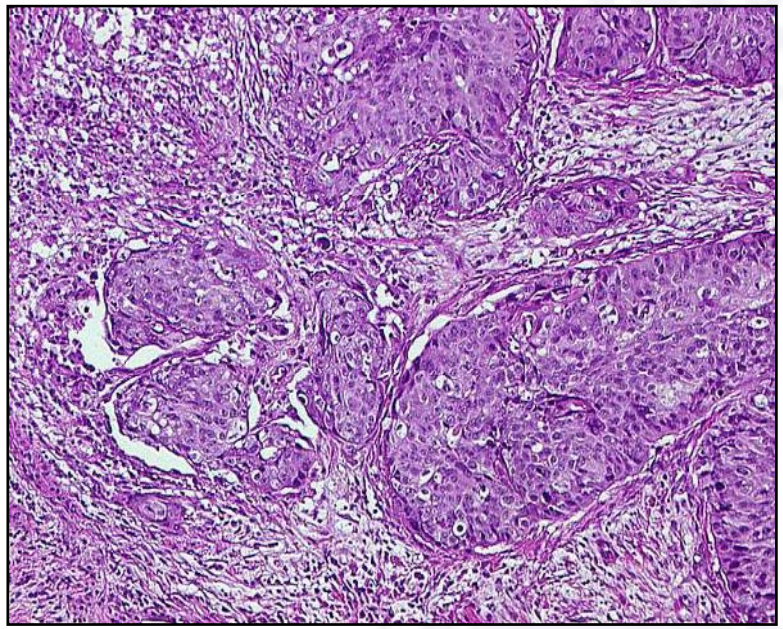

Fig. 2c: Irregular infiltrates of tumor cells in connective tissue with inflammatory reaction.

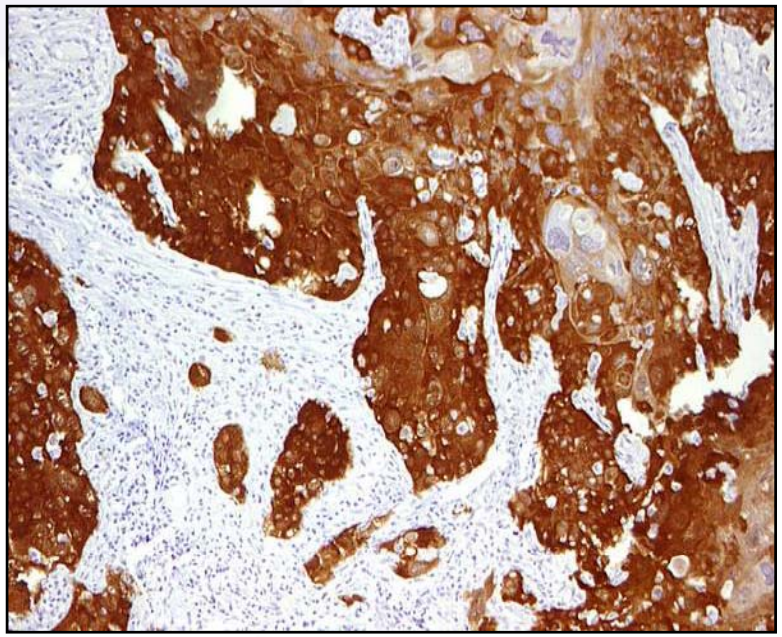

Fig. 2d: Strong cytoplasmic and nuclear positivity for $p16^{INK4a}$ of carcinoma cells.

Endocervical adenocarcinoma (in situ)

Tumor cells of endocervical adenocarcinoma in situ: Fig. 3a: Pseudostratified complex of malignant glandular cells with marked nuclear enlargement and “feathering“ (here:Endocervical adenocarcinoma in situ).

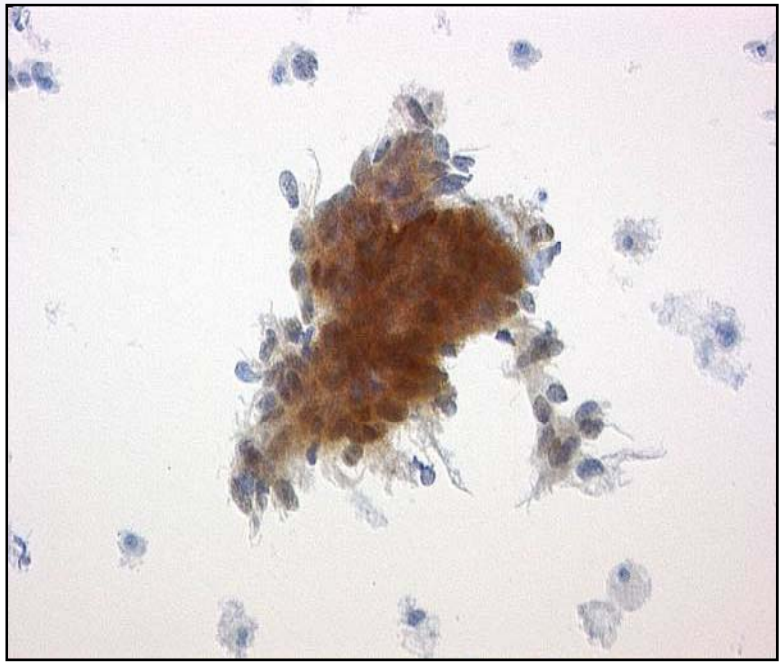

Tumor cells of endocervical adenocarcinoma: Fig. 3b: Strong positivity for $p16^{INK4a}$ in cytoplasm and nuclei of malignant glandular cells.

Endocervical adenocarcinoma

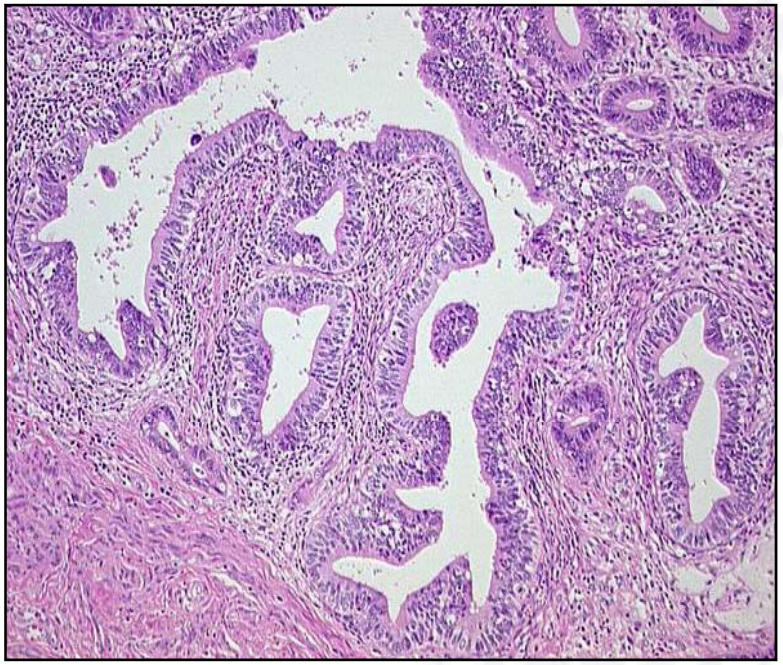

Endocervical adenocarcinoma (Grade I):
Fig. 3c: Neoplastic endocervical glands are lined by a pseudostratified epithelium, consisting of neoplastic columnar cells with hyperchromatic, irregularly shaped nuclei.

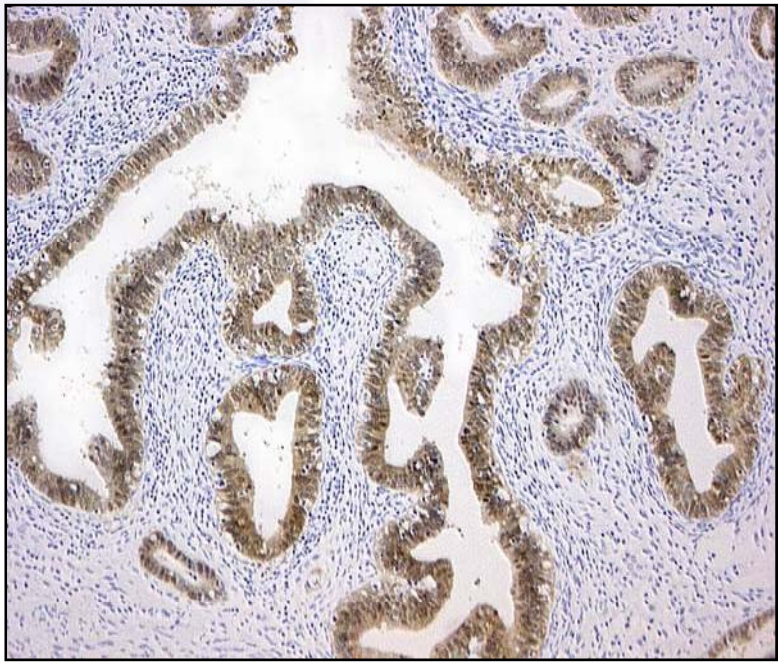

Endocervical adenocarcinoma (Grade I):
Fig. 3d: Strong cytoplasmic and nuclear positivity for $p16^{INK4a}$ with a diffuse distribution.

Cervical Intraepithelial Neoplasia Grade 3

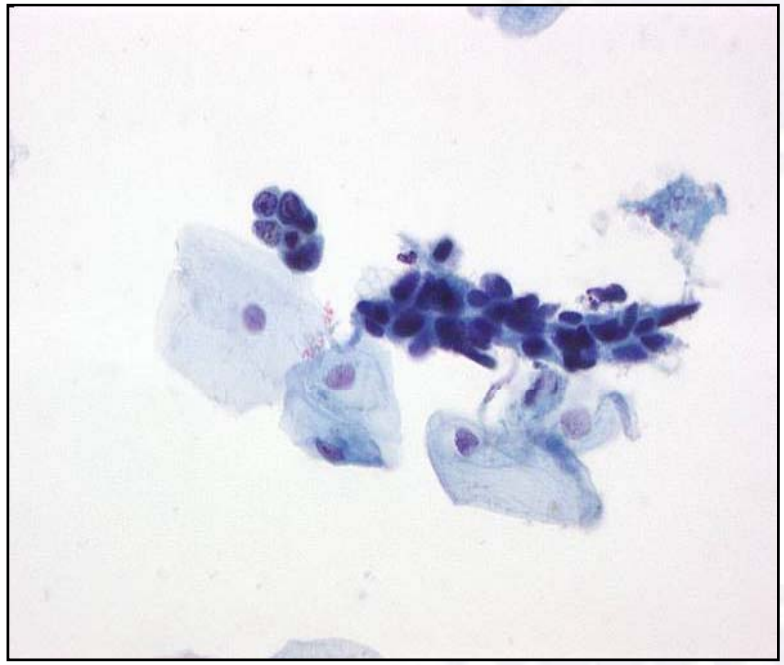

Cells from CIN3 (HSIL): Fig. 4a:
Several undifferentiated neoplastic cells. Marked hyperchromasia and anisonucleosis. Marked increase of nuclear-cytoplasmic ratio.

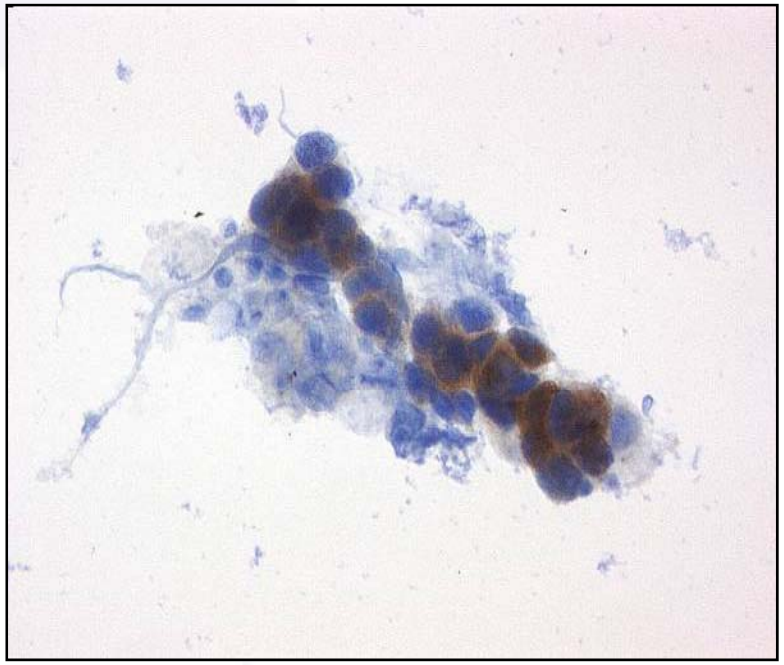

Cells from CIN3 (HSIL): Fig. 4b: Strong cytoplasmic and nuclear positivity for $p16^{INK4a}$.

Cervical Intraepithelial Neoplasia Grade 3 (Carcinoma in situ)

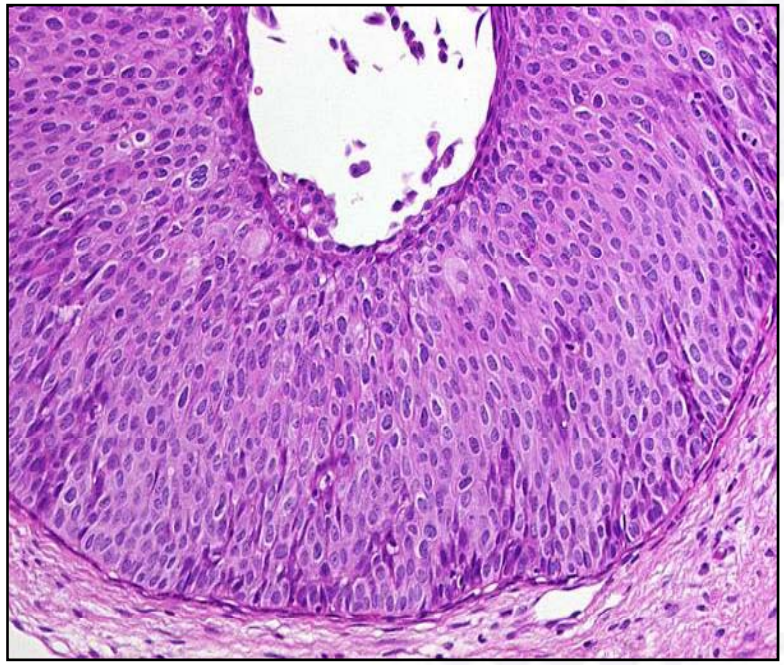

Carcinoma in situ (CIN3): Fig. 5a: (Carcinoma in situ) extending into endocervical gland. Neoplastic cells with relatively uniform, hyperchromatic nuclei throughout the epithelium.

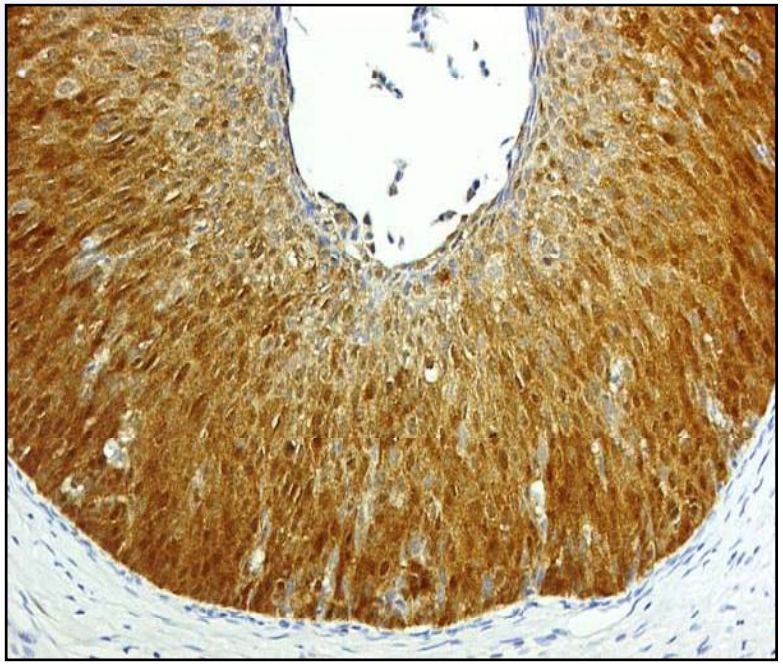

Carcinoma in situ (CIN3): Fig. 5b: Carcinoma in situ extending into endocervical gland. Strong nuclear and cytoplasmic $p16^{INK4a}$ positivity in neoplastic epithelium in a diffuse distribution.

Cervical Intraepithelial Neoplasia Grade 3 (Severe Dysplasia)

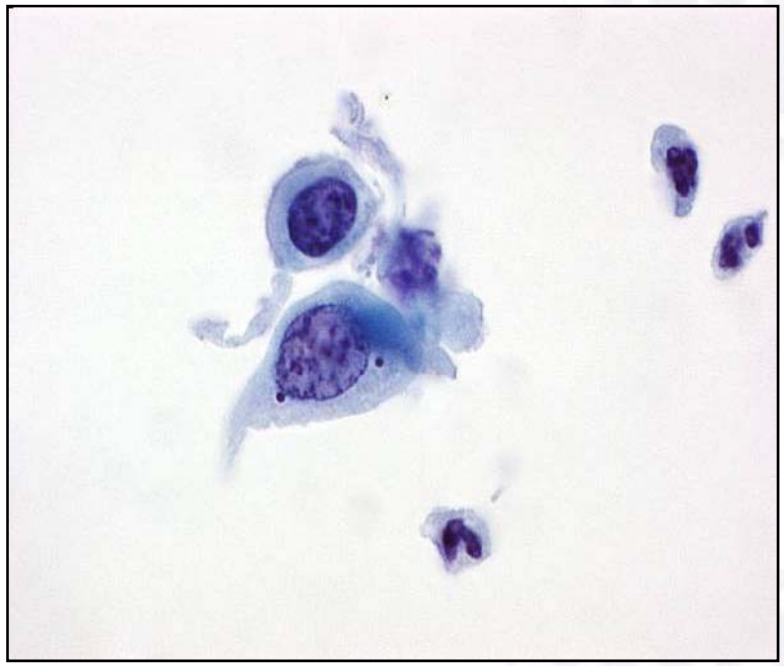

Dysplastic cells from severe dysplasia (HSIL):
Fig. 6a: Dysplastic cells with variation of nuclear and cytoplasmic shape. Markedly increased nuclear-cytoplasmic ratio. Coarsely granular chromatin. No nuceoli.

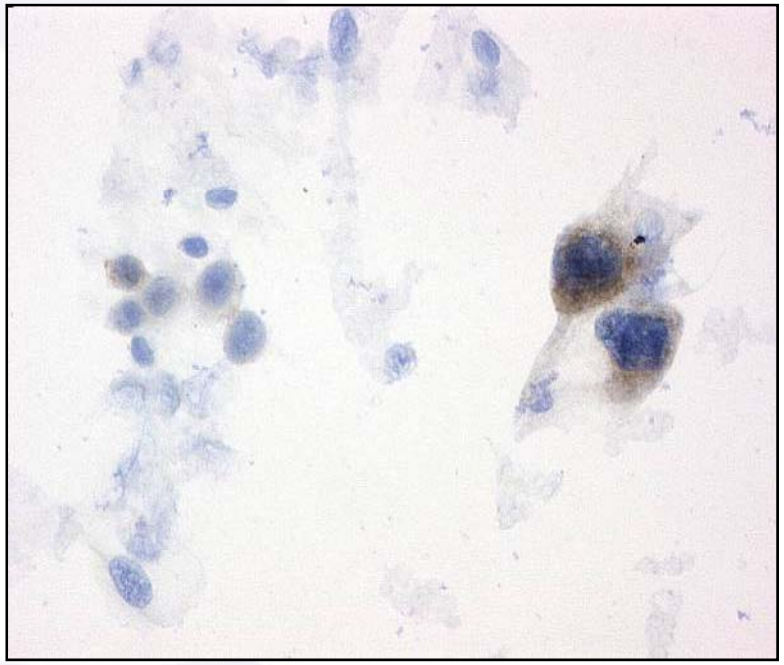

Dysplastic cells from severe dysplasia (HSIL):
Fig. 6b: Nuclear and cytoplasmic positivity for $p16^{INK4a}$.

Cervical Intraepithelial Neoplasia Grade 3 (Severe Dysplasia)

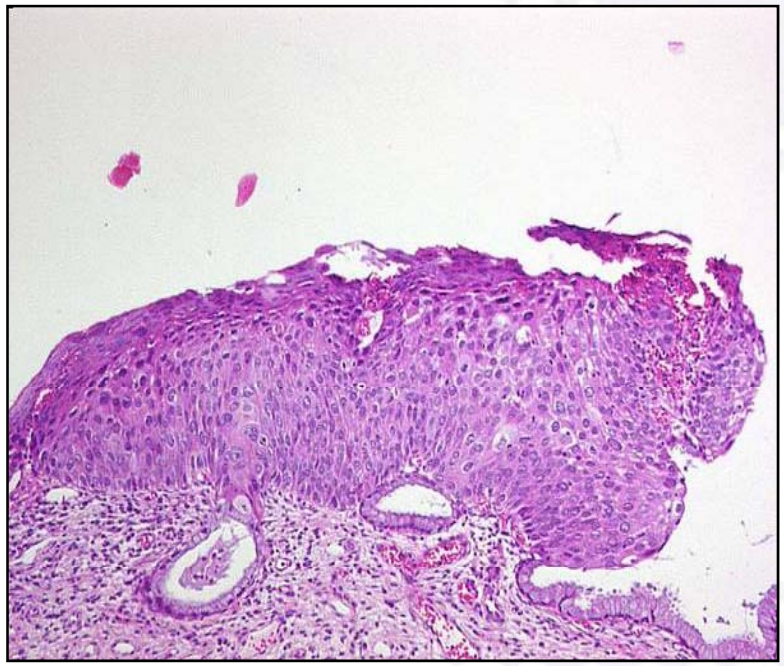

Severe dysplasia (CIN3)Fig. 6c: Dysplastic cells with large, hyperchromatic nuclei almost throughout the entire epithelium.

Severe dysplasia (CIN3) Fig. 6d: Mostly strong, nuclear and cytoplasmic positivity for $p16^{INK4a}$ in dysplastic epithelium with a diffuse distribution.

Cervical Intraepithelial Neoplasia Grade 2

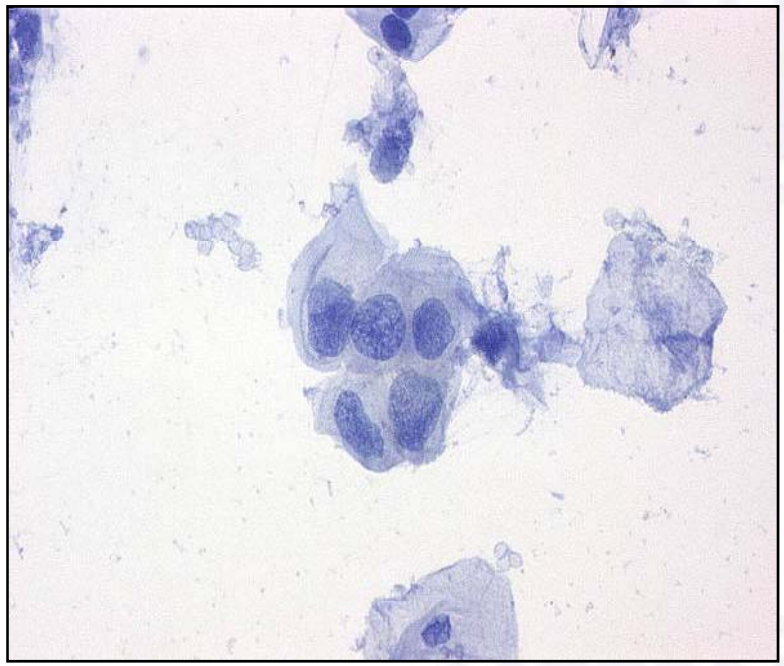

Cells from CIN2 (HSIL):
Fig. 7a: Sheet of dysplastic cells of intermediate cell layers. Variation of nuclear shape. Nuclear enlargement. Coarsely granular chromatin. Chromocenters. No nucleoli. No $p16^{INK4a}$ positivity.

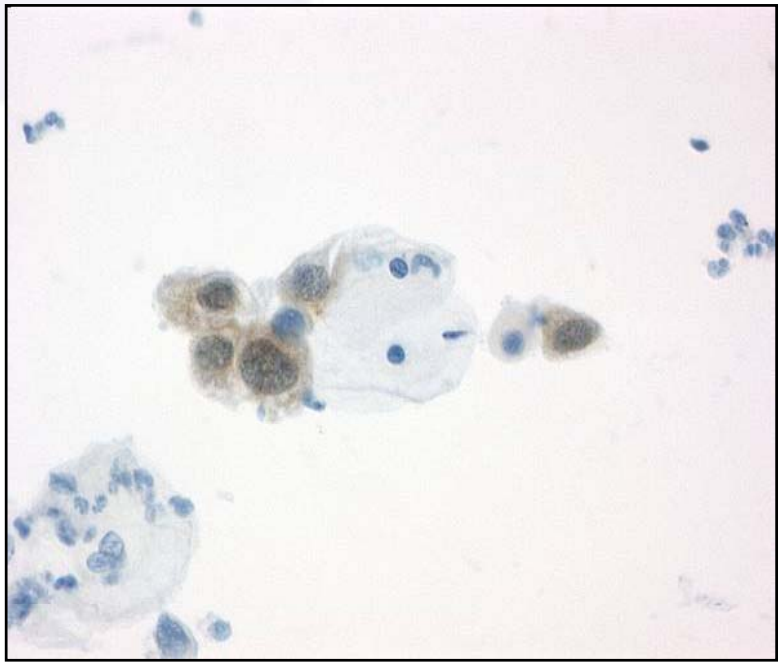

Cells from CIN2 (HSIL):
Fig. 7b: Several dysplastic cells of deeper layers. Marked variation of nuclear and cytoplasmic shape. Increased nuclear-cytoplasmic ratio. Hyperchromasia. Coarsely granular chromatin. Cytoplasmic and nuclear positivity for $p16^{INK4a}$ in dysplastic cells.

Cervical Intraepithelial Neoplasia Grade 2

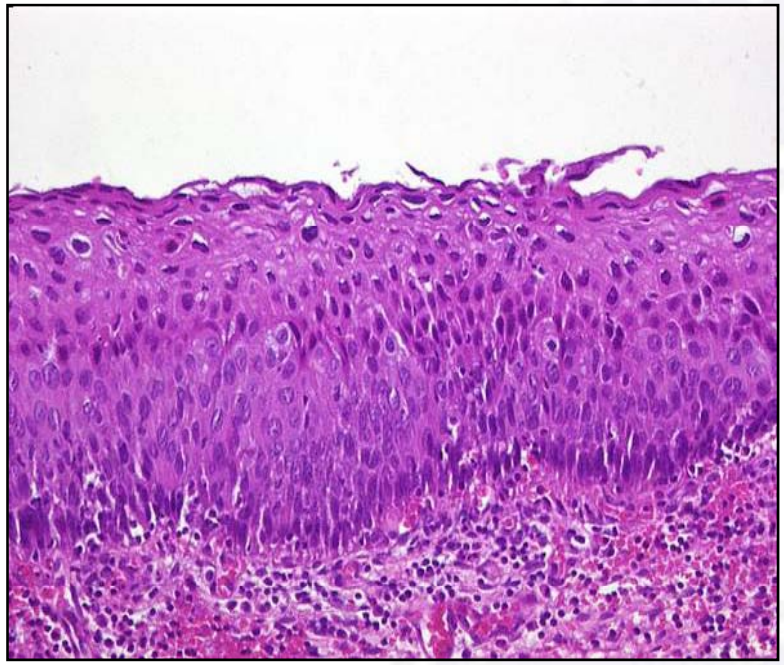

CIN2 without koilocytosis:
Fig. 7c: Dysplastic cells in the lower half of the epithelium.

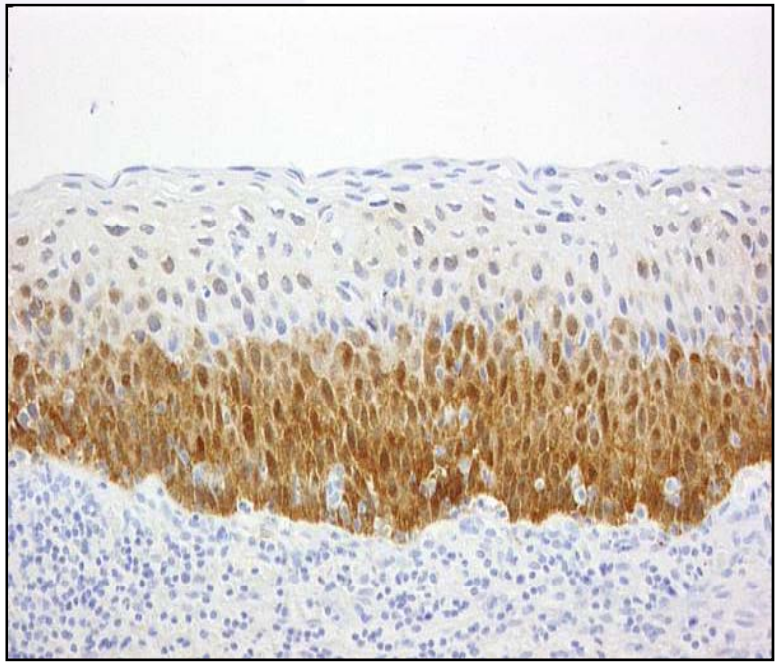

CIN2 without koilocytosis:
Fig. 7d: In the lower half of the epithelium dysplastic cells show cytoplasmic and nuclear $p16^{INK4a}$ positivity in a diffuse distribution. The cells in the superficial layers show no or only weak $p16^{INK4a}$ positivity.

Koilocytosis

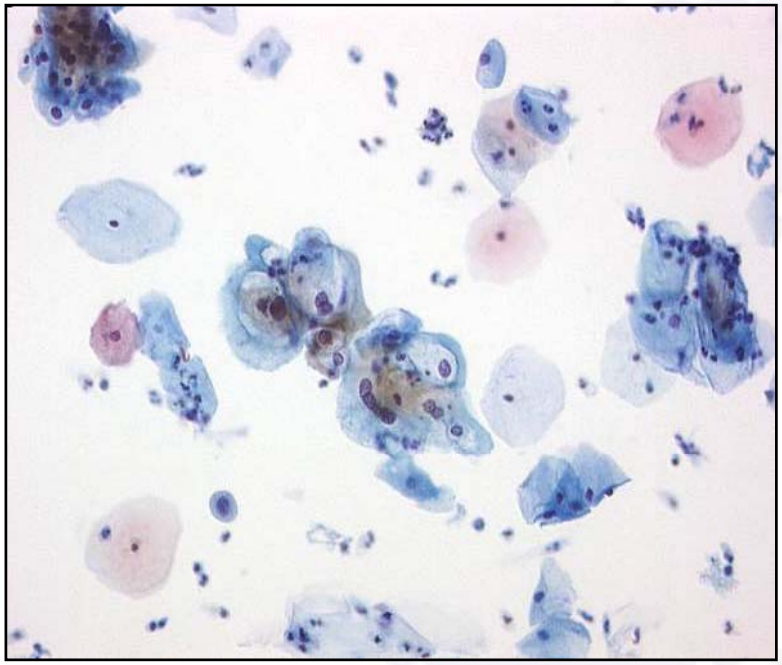

Koilocytes:
Fig. 8a: Large intermediate cells with perinuclear cavity. Relatively dense rim of peripheral cytoplasm. Mild nuclear irregularity with hyperchromasia.

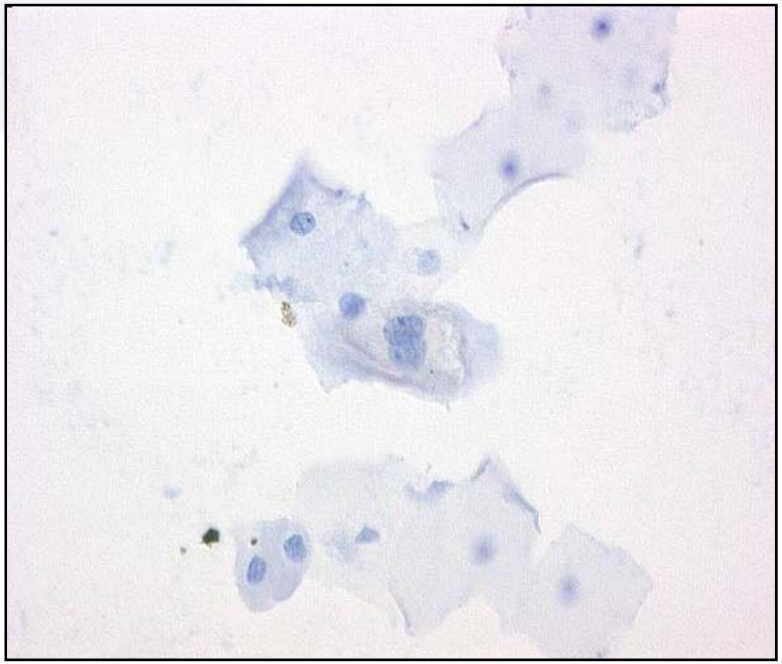

Koilocyte:
Fig. 8b: No staining reaction for $p16^{INK4a}$ in koilocyte with a double nucleus.

Koilocytosis

CIN2 with Koilocytosis:
Fig. 8c: Moderate dysplasia showing koilocytes with perinuclear cavity and mildly irregular, hyperchromatic nuclei in upper epithelial cell layers (Arrowhead: Mitosis).

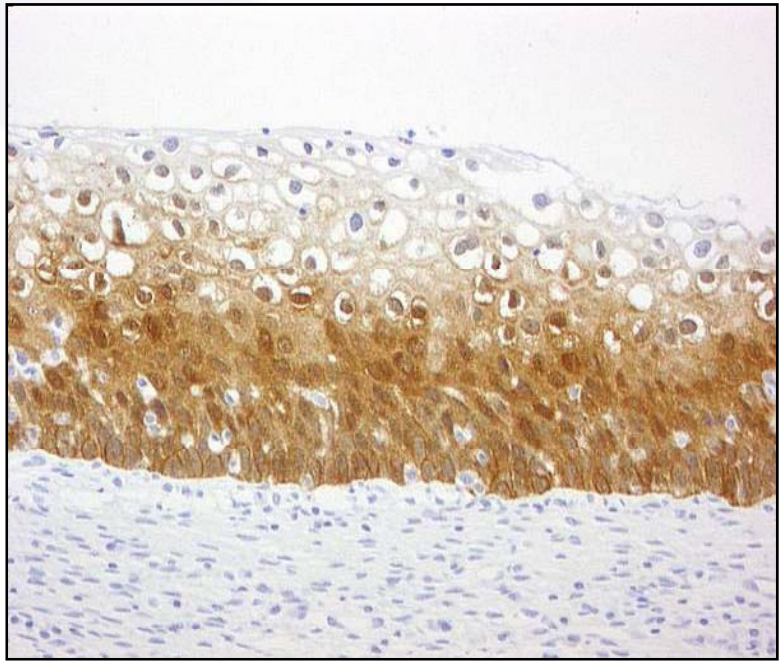

CIN2 with koilocytosis:
Fig. 8d: $p16^{INK4a}$ positivity only in dysplastic cells of basal and parabasal layers, koilocytes in upper layers are mostly $p16^{INK4a}$ negative.

Normal maturation of stratified squamous epithelium

p16^{INK4a} immunostain: no positive cells

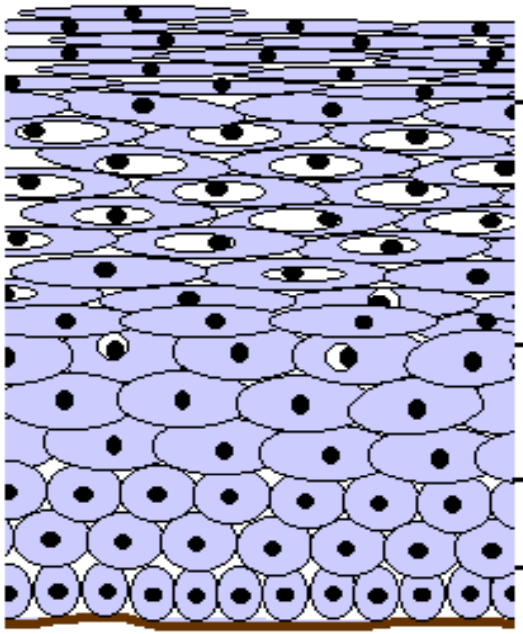

Superficial cells	Terminally differentiated cells
Large intermediate cells with glycogen vacuoles	Differentiating cells
Small intermediate cells	Commitment to terminal differentiation
Parabasal cells	Transient amplifying cells
Basal cells	Stem cell compartment

Fig. 9: Scheme of p16^{INK4a} immunostaining, stratified squamous epithelium

Superficial cells

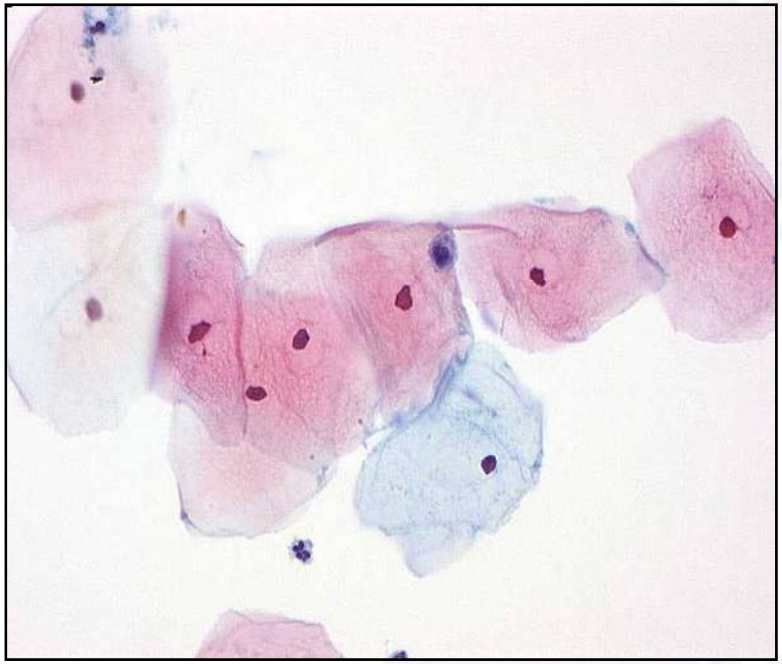

Superficial cells from stratified squamous epithelium: Fig. 10a: Large polygonal flat cell. Distinct cell borders. Pyknotic nuclei.

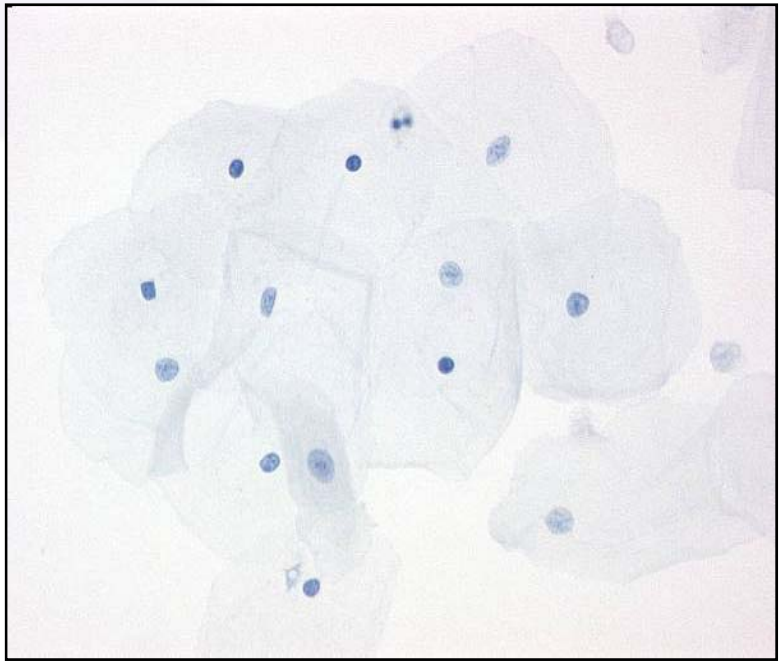

Superficial cells from stratified squamous epithelium: Fig. 10b: Negative for p16INK4a.

Squamous epithelium, upper layers

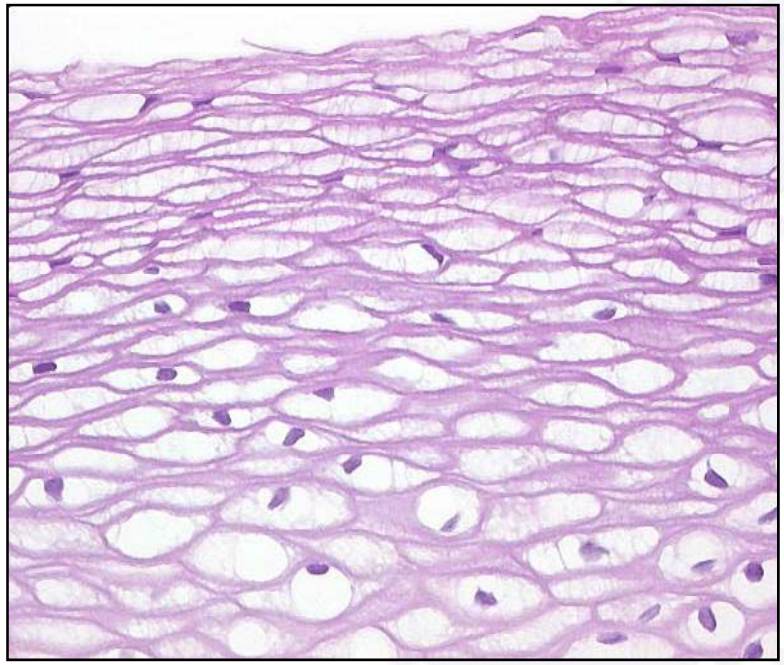

Normal stratified squamous epithelium, superficial cell layers:
Fig. 11 a: Superficial differentiated squamous cells with large and flat cell bodies. Pyknotic nuclei.

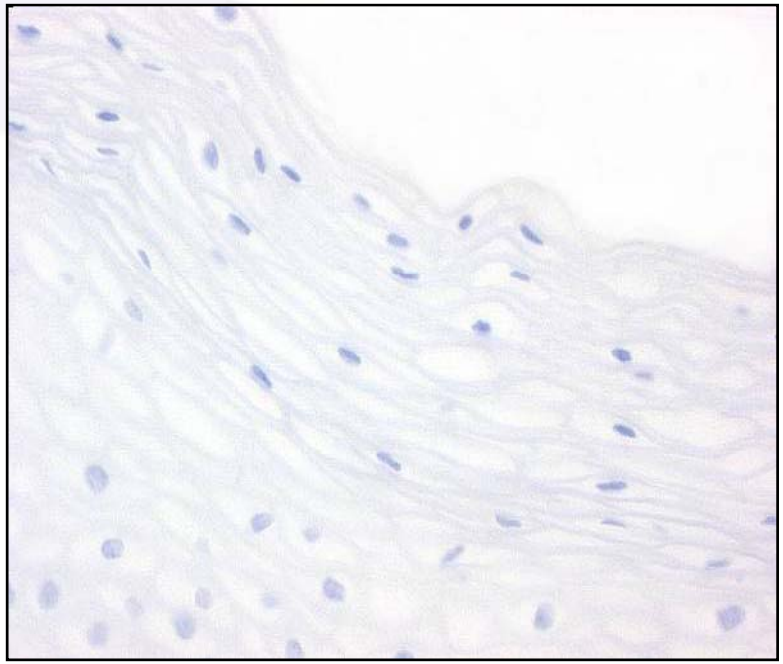

Normal stratified squamous epithelium, superficial cell layers:
Fig. 11b: Negative for $p16^{INK4a}$.

Squamous epithelium, intermediate layers

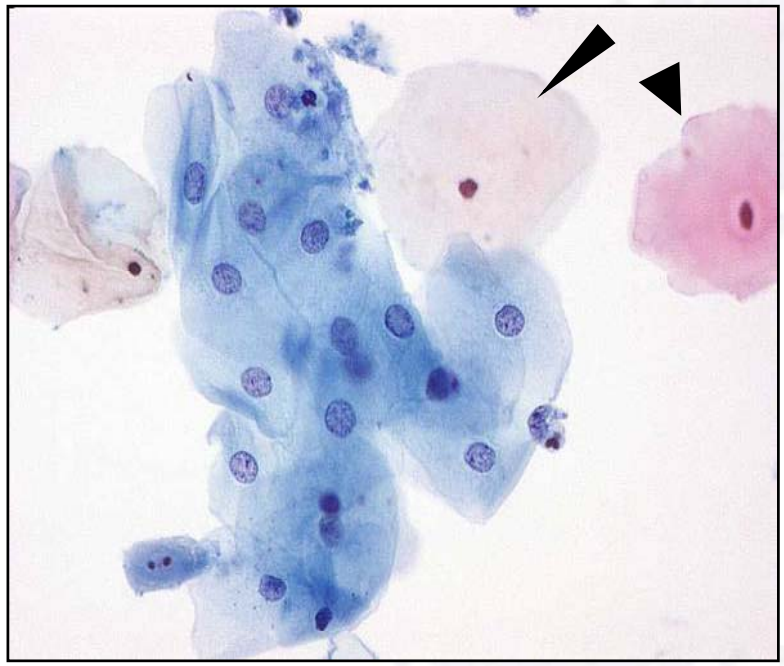

Intermediate cells from stratified squamous epithelium:
Fig. 12a: Large to medium large polygonal cells. Distinct cell borders. Vesicular nuclei. Finely granular chromatin. Occasionally chromocenters. Open arrowheads: Superficial cells.

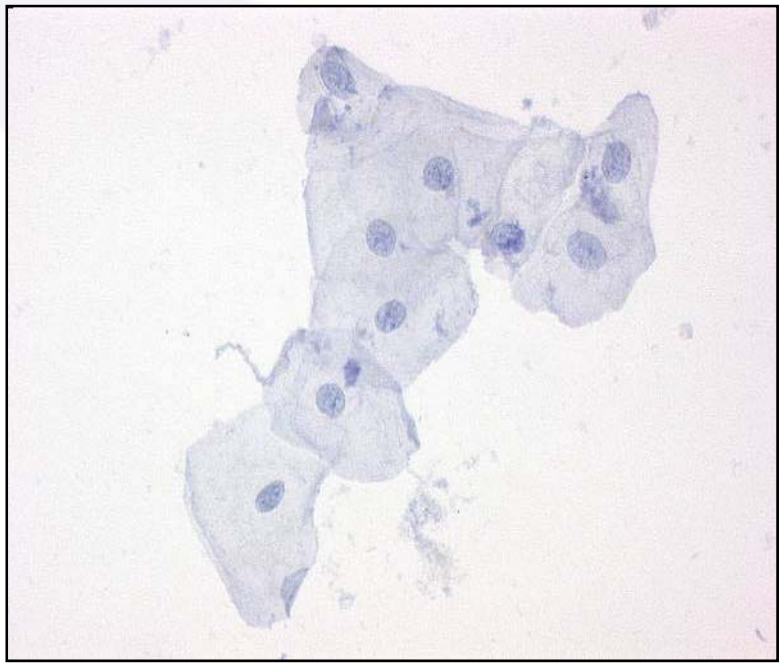

Intermediate cells from stratified squamous epithelium:
Fig. 12b: Negative for $p16^{INK4a}$.

Squamous epithelium, intermediate layers

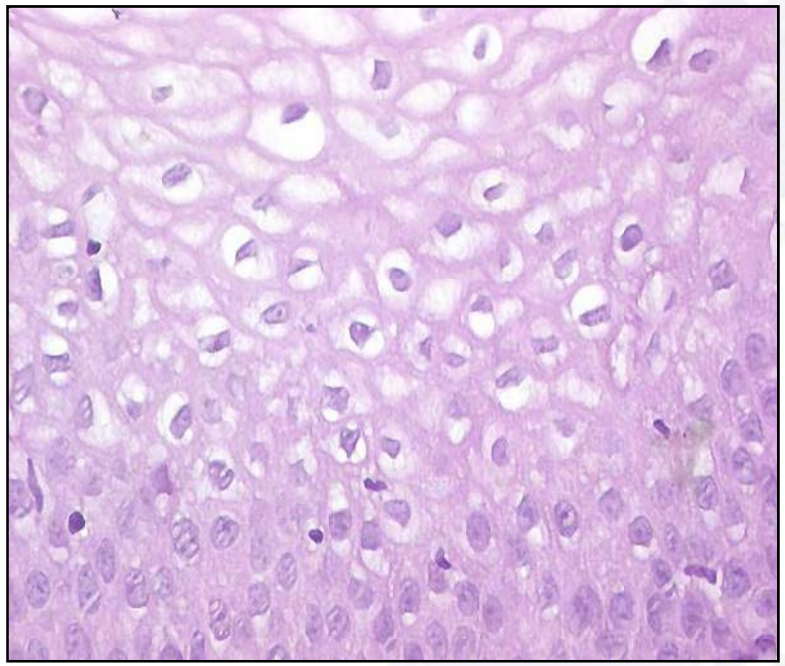

Stratified squamous epithelium, intermediate cell layer: Fig. 12c: Medium large, differentiating polygonal cells. Vesicular nuclei. Uniformely fine granular chromatin. Vacuolic cell body due to glycogen content.

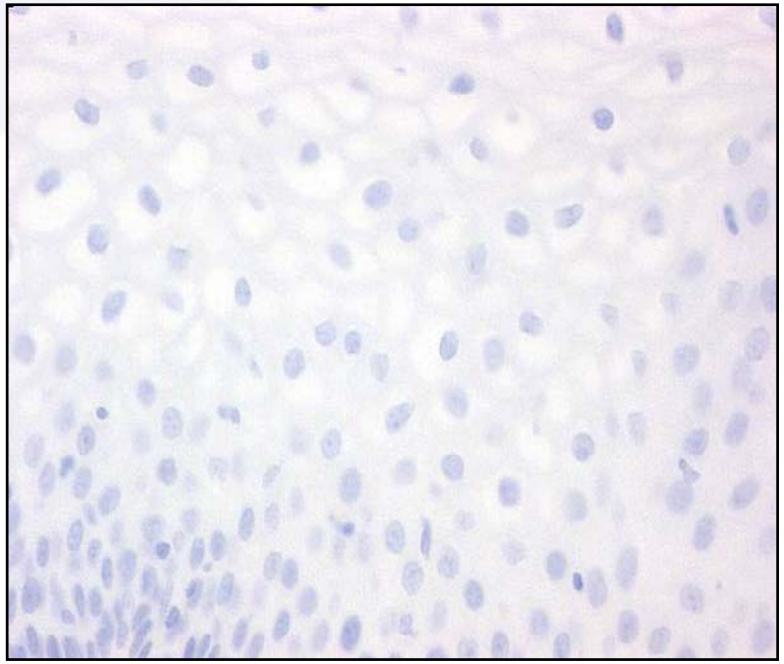

Stratified squamous epithelium, intermediate cell layer: Fig. 12d: Negative for $p16^{INK4a}$.

Squamous epithelium, parabasal cells

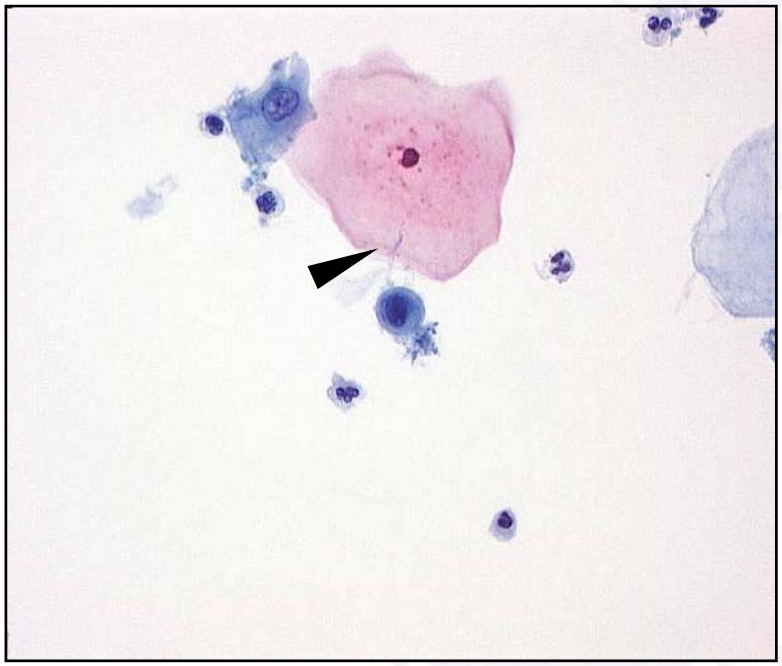

Parabasal cells from stratified squamous epithelium:
Fig. 13a: Relatively small squamous cells with round to oval shape. Round to oval vesicular nuclei. Evenly distributed and finely granular chromatin. Chromocenters.

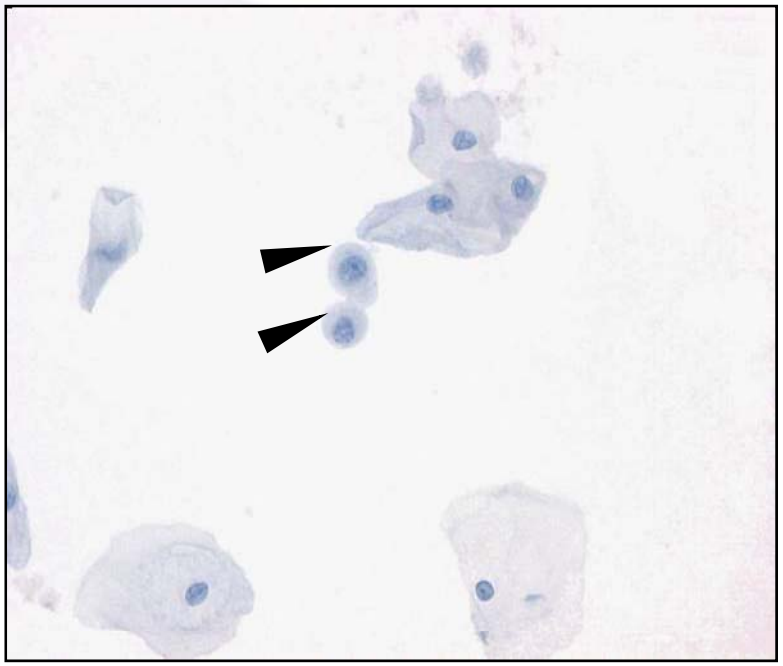

Parabasal cells from stratified squamous epithelium:
Fig. 13b: Negative for p16INK4a.

Squamous epithelium, lower layers

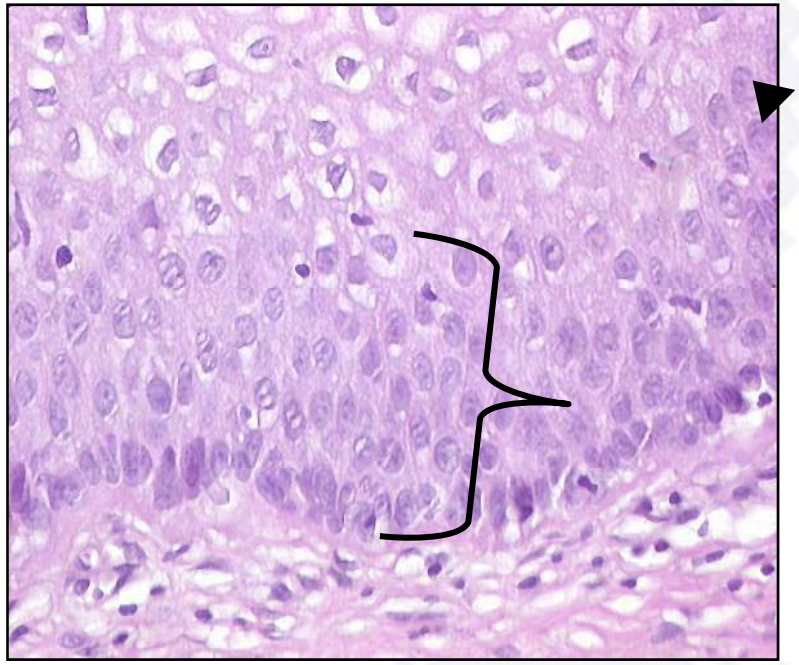

Stratified squamous epithelium, basal and parabasal cell layer:
Fig. 14a: Relatively small squamous cells with round to oval shape. Round to oval vesicular nuclei. Arrowhead: Clearly delineated row of palisading basal cells. Bracket: Parabasal cell layers.

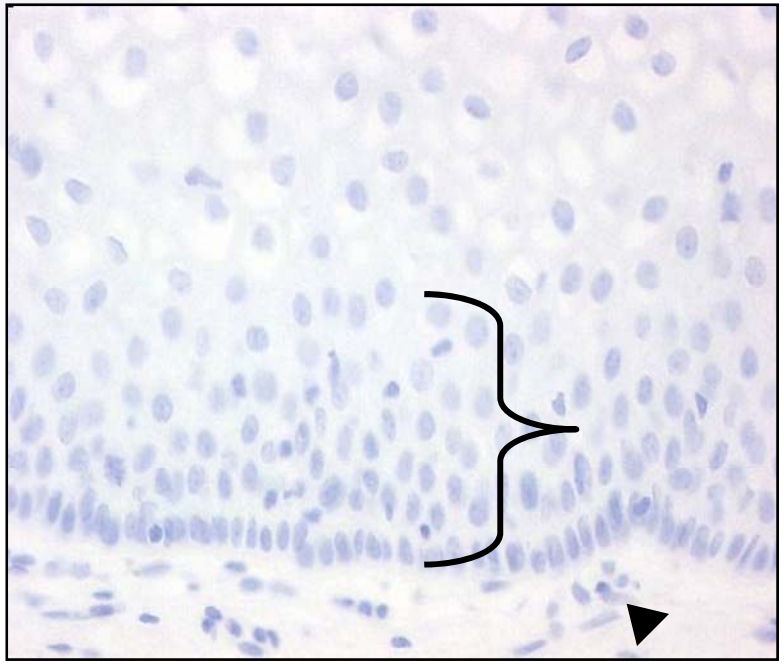

Stratified squamous epithelium, basal and parabasal cell layer:
Fig. 14b: Negative for $p16^{INK4a}$. Arrowhead: Clearly delineated row of palisading basal cells. Bracket: Parabasal cell layers.

Atrophy

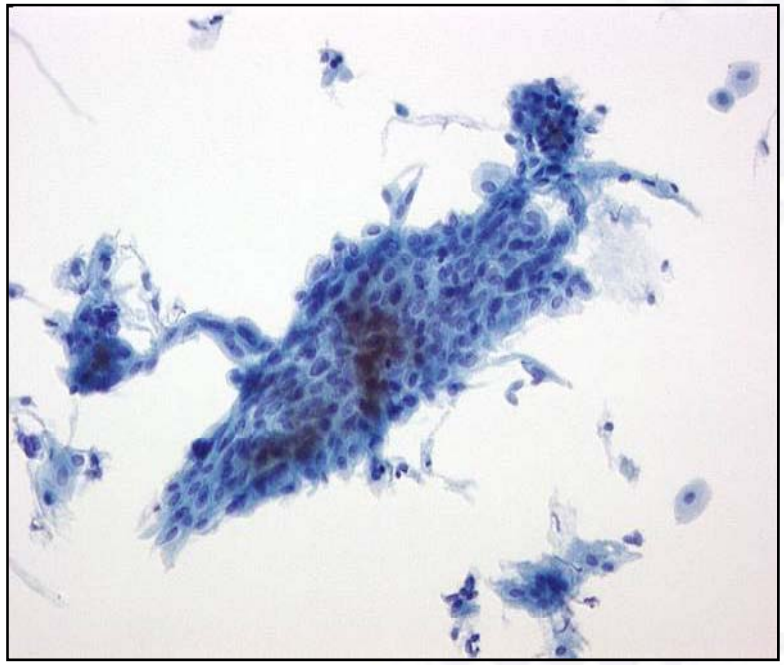

Cells from ectocervical atrophy:
Fig. 15a: Atrophic cell cluster, small rounded to slightly elongated cells with small round to oval regular nuclei, some of them slightly hyperchromatic. Some small intermediate cells.

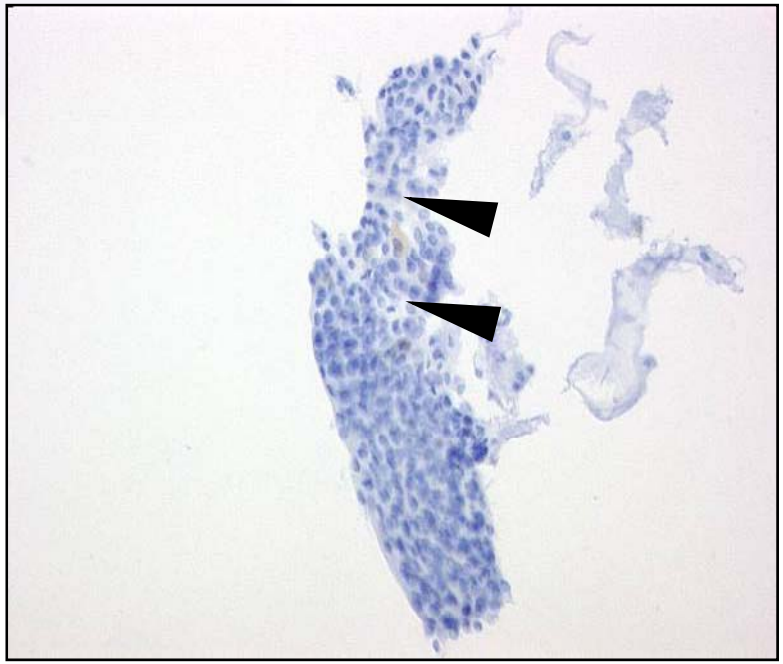

Cells from ectocervical atrophy:
Fig. 15b: Negative for p16INK4a with occasional positive cells in superficial layers (Arrowheads).

Squamous epithelium, Atrophy

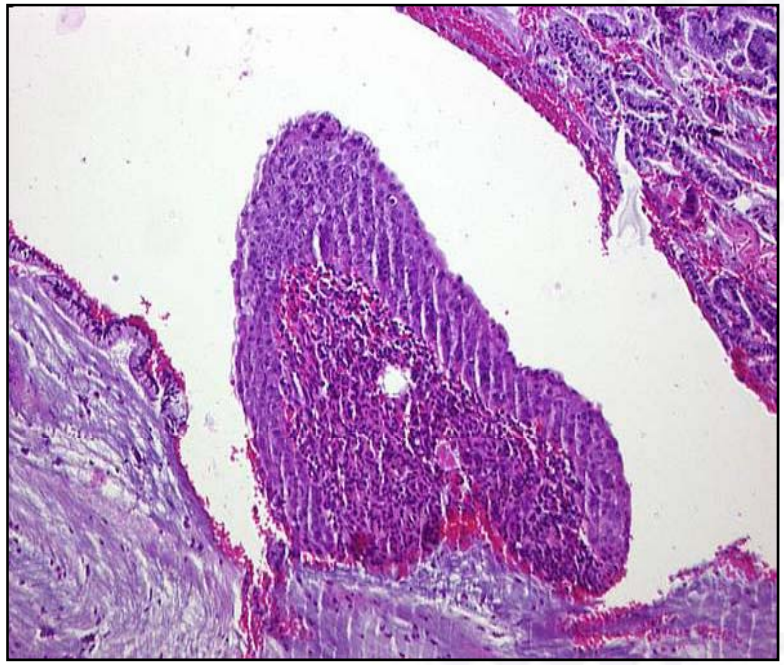

Atrophic squamous epithelium:
Fig. 16a: Stratified squamous epithelium with little maturation. Epithelium is composed almost entirely of basal and parabasal cells.

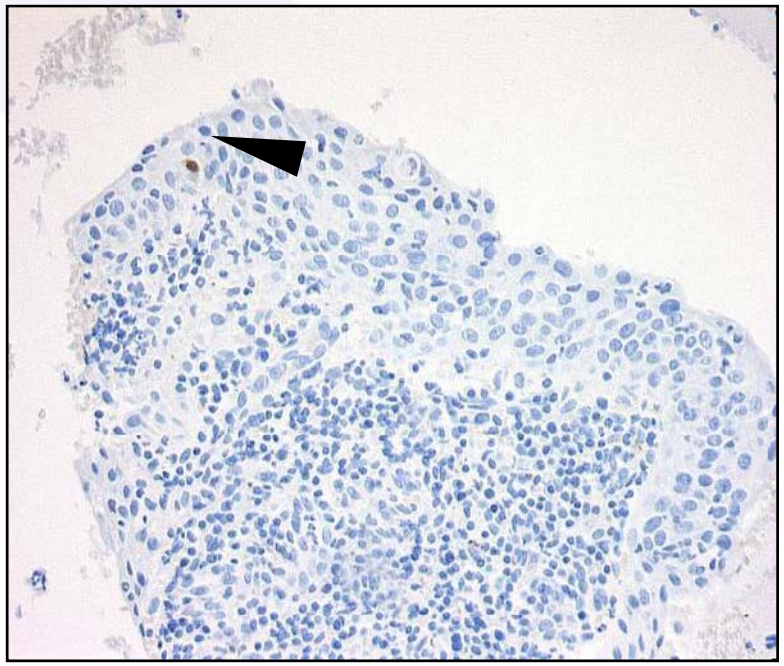

Atrophic squamous epithelium:
Fig. 16b: Negative for $p16^{INK4a}$ with occasional positive cells in superficial layers (Arrow).

Endocervical columnar cells

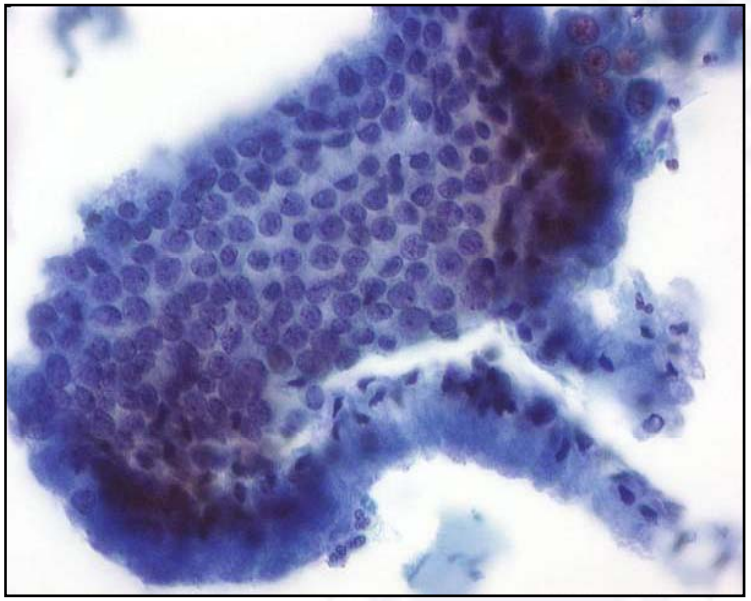

Columnar cells from endocervical epithelium:
Fig. 17a : Mucus producing cells in palisading and also in honeycomb arrangement. Distinct cell borders. Round to oval, basally located nuclei of uniform size. Finely granular chromatin. Chromocenters.

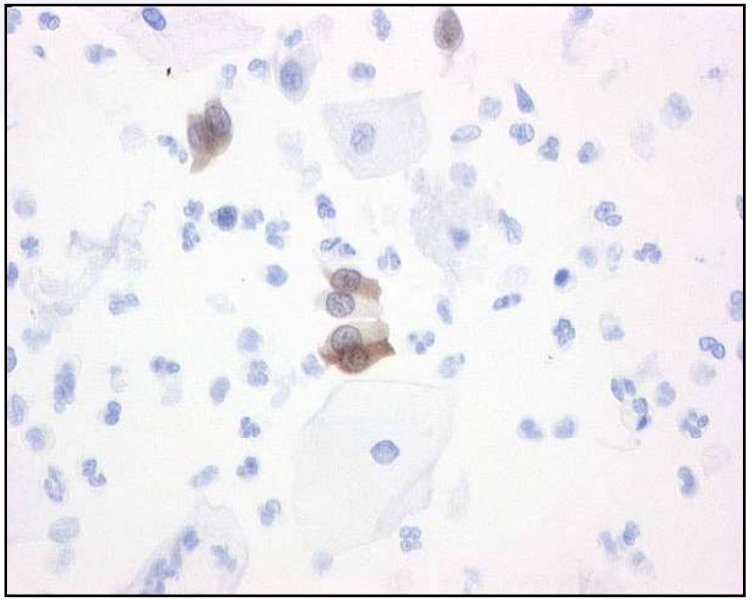

Columnar cells from endocervical epithelium:
Fig. 17b: Single layered endocervical cells, columnar cells mostly negative for p16INK4, occasionally a positive p16INK4a reaction in cytoplasm and nuclei of columnar cells is seen.

Endocervical epithelium

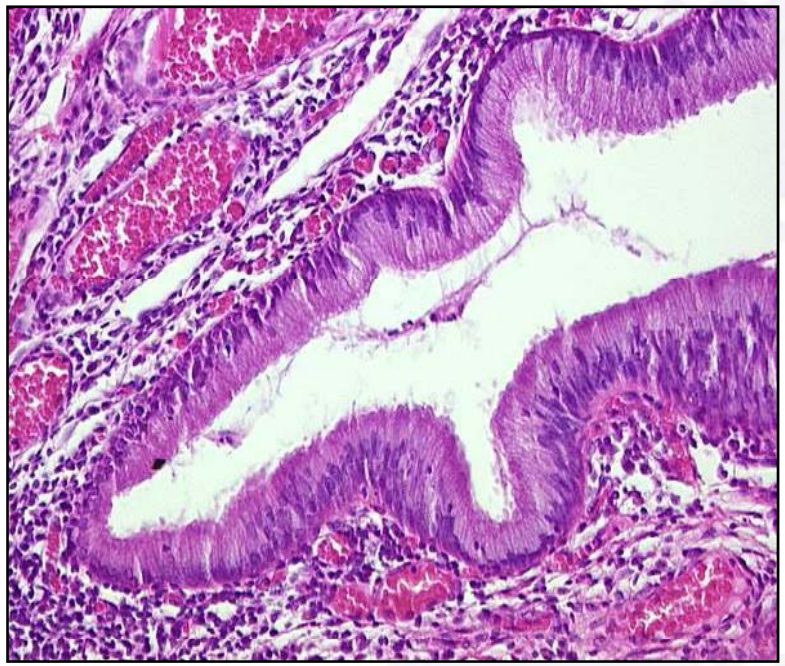

Endocervical mucosa, columnar cells:
Fig. 18a: Mucus producing cells in a single layer lining an endocervical gland. Distinct cell borders. Round to oval, basally located nuclei of uniform size. Mucus in glandular lumen.

Endocervical mucosa, columnar cells:
Fig. 18b: Overwhelming majority of cells negative for $p16^{INK4}$, interspersed single cells may occasionally show positive $p16^{INK4a}$ reaction in cytoplasm and nuclei.

Endometrium

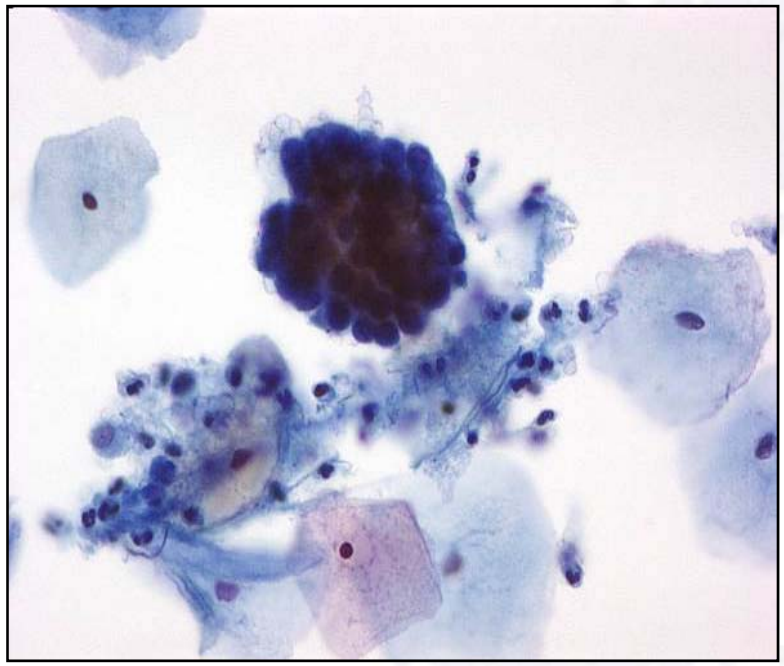

Cluster of endometrial cells:
Fig. 19a: Three-dimensional cluster of endometrial cells with rounded outline from the endometrial cavity. Tightly packed nuclei, obscuring nuclear detail. Round to oval nuclear shape. Uniformely fine chromatin. Chromocenters.

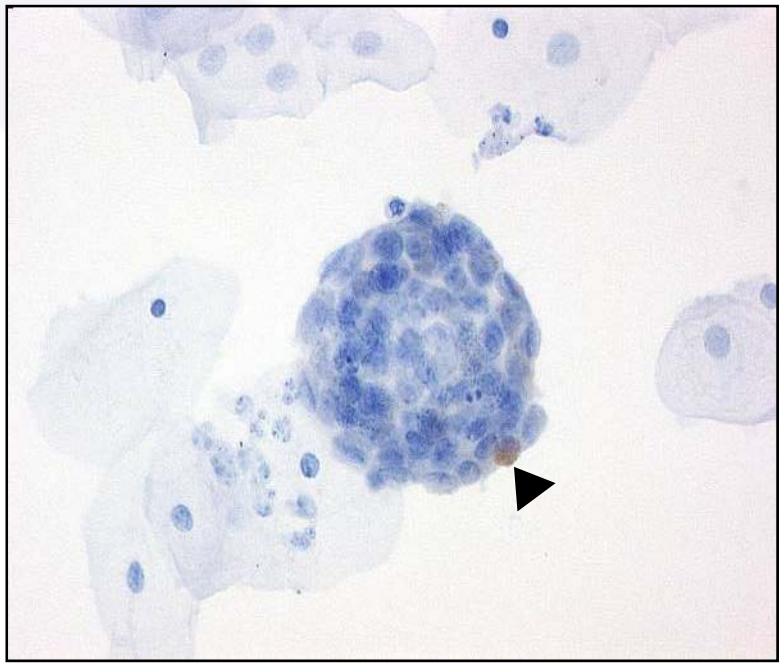

Fig. 19b: Single cells positive for p16INK4a.

Endometrium

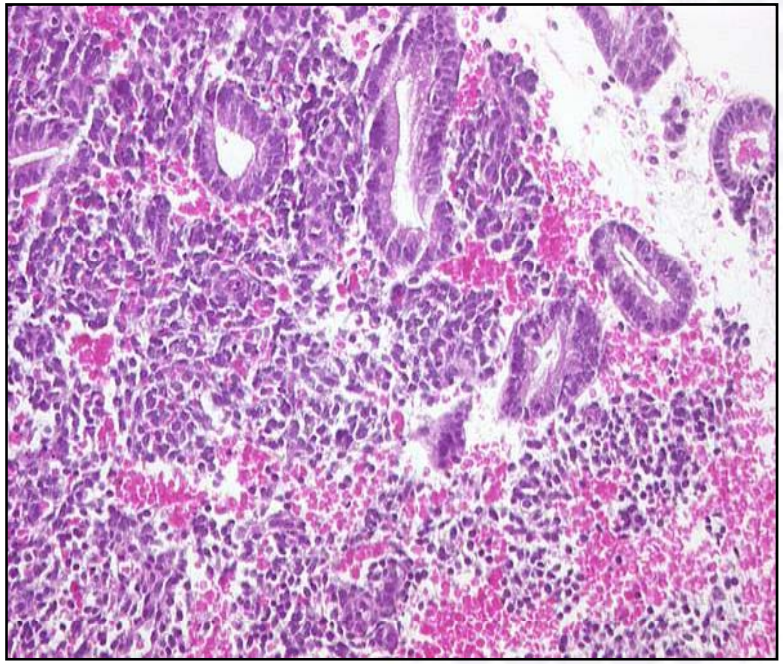

Endometrium during menstruation:
Fig. 19c: Glands and stromal cells of endometrial tissue shrunken and partly dissociated with cellular aggregates between fresh hemorrhages.

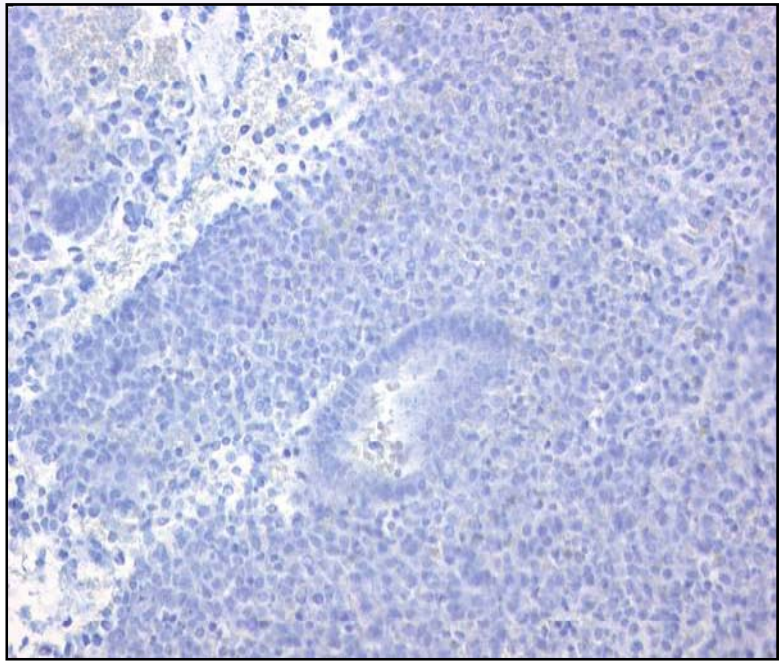

Endometrium during menstruation:
Fig. 19d: Single cells may occasionally show $p16^{INK4a}$ positivity.

Inflammation

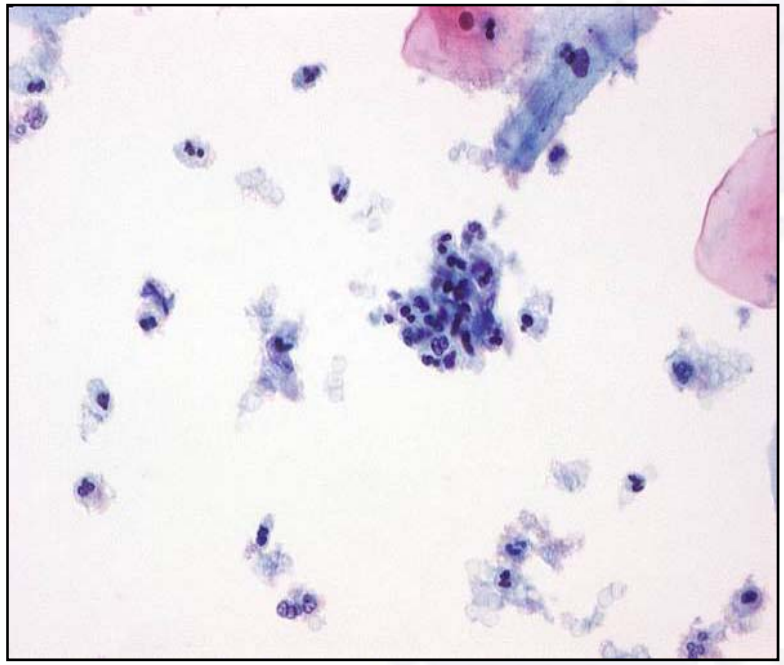

Neutrophil granulocytes:
Fig. 20a: Polymorphonuclear leukocytes with typical nuclear shape.

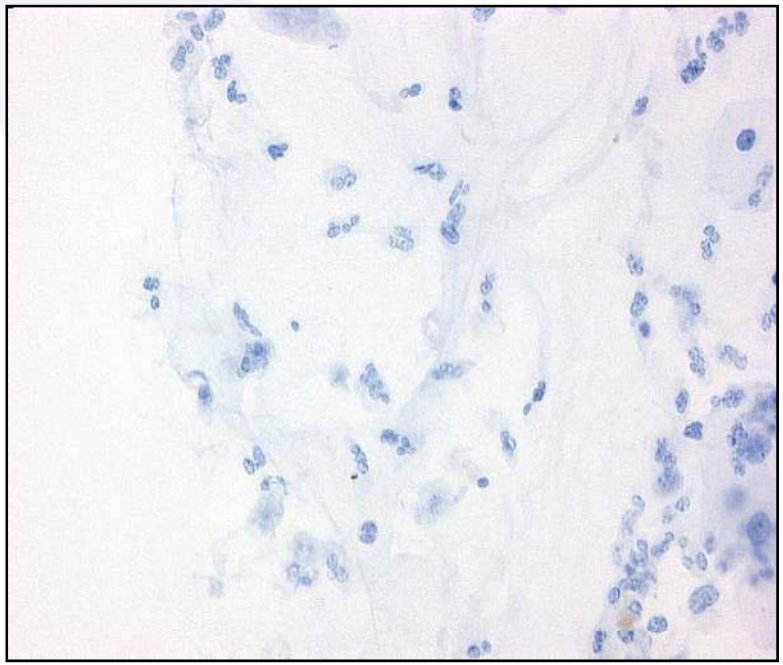

Neutrophil granulocytes:
Fig. 20b: Negative for p16INK4a.

Inflammation

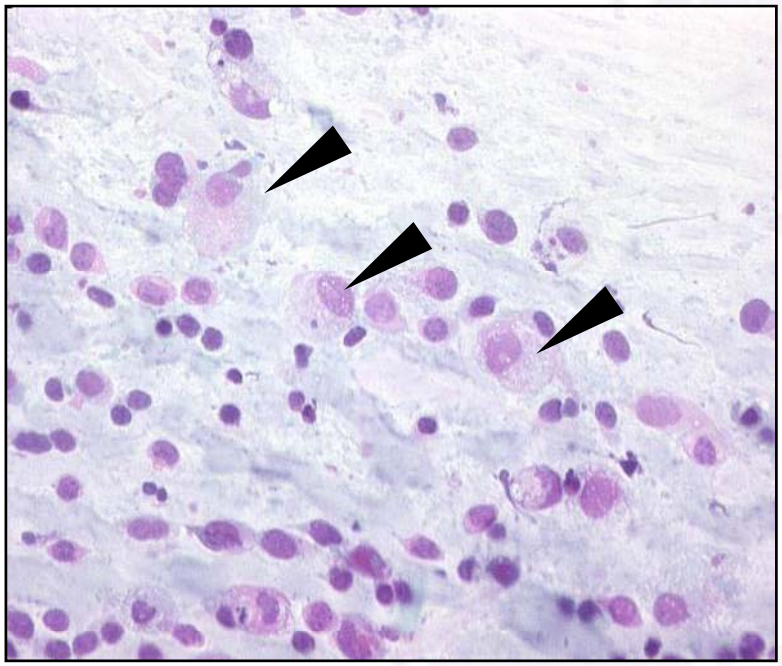

Histiocytes:
Fig. 20c: Open arrowheads: Several large histiocytes with typical foamy cytoplasm and indistinct cell borders (conventional smear).

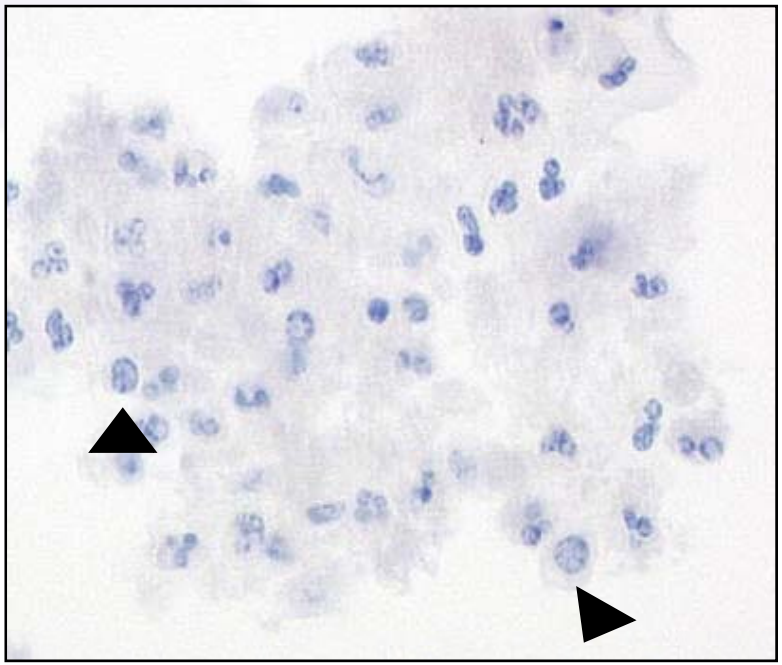

Histiocytes:
Fig. 20d: Open arrowheads: Histiocytes are negative for $p16^{INK4a}$.

Microorganisms

Bacteria:
Fig. 21a: Small rod-shaped bacteria of Döderlein type.

Fig. 21b: Positive staining reaction of bacteria in less than 5% of the cases, always easily discriminated from cellular staining.

Microorganisms

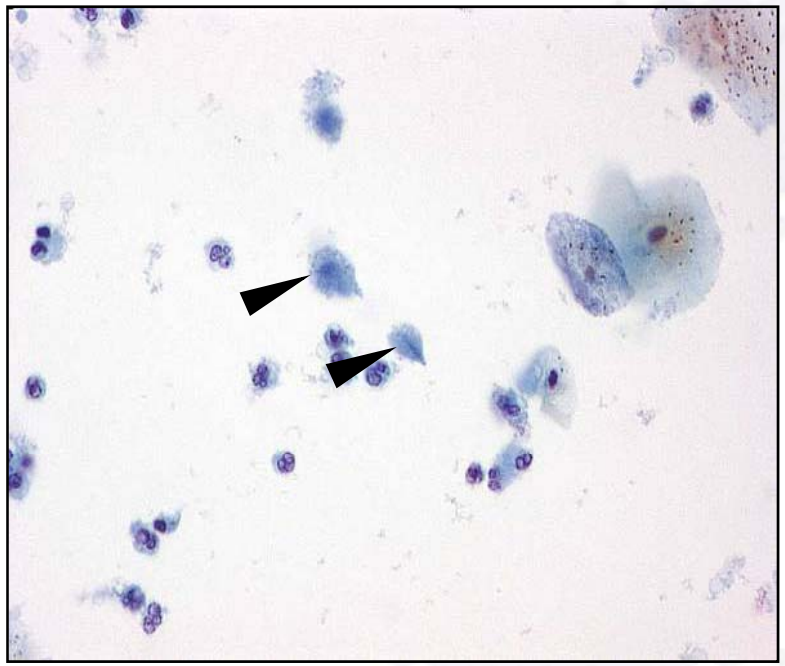

Trichomoniasis:
Fig. 21c: Oval to pear shaped trichomonads with flagelli. Small, comma-shaped nucleus. Some granulocytes.

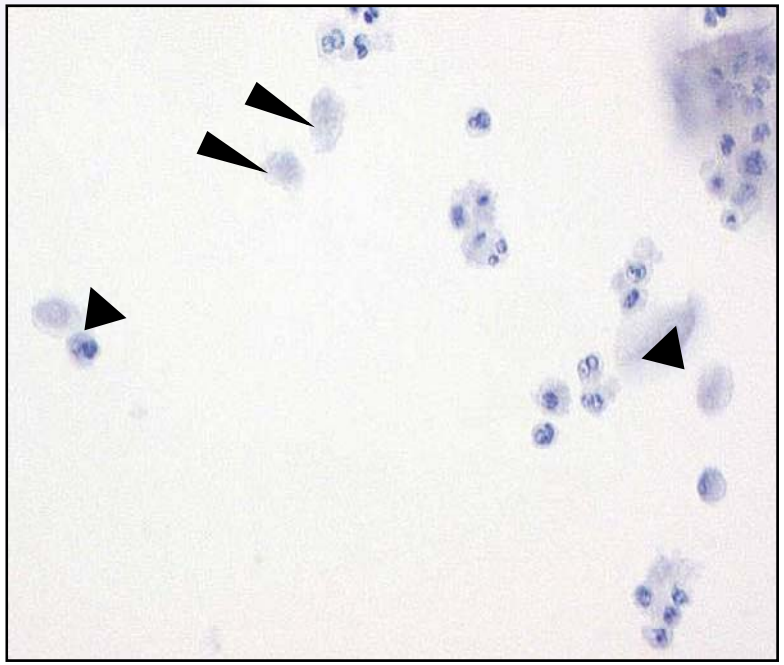

Trichomoniasis:
Fig. 21d: Negative staining reaction with CINtec® Cytology Kit. Staining with other antibodies against the antigen $p16^{INK4a}$ may result in false-positive reaction.

Microorganisms

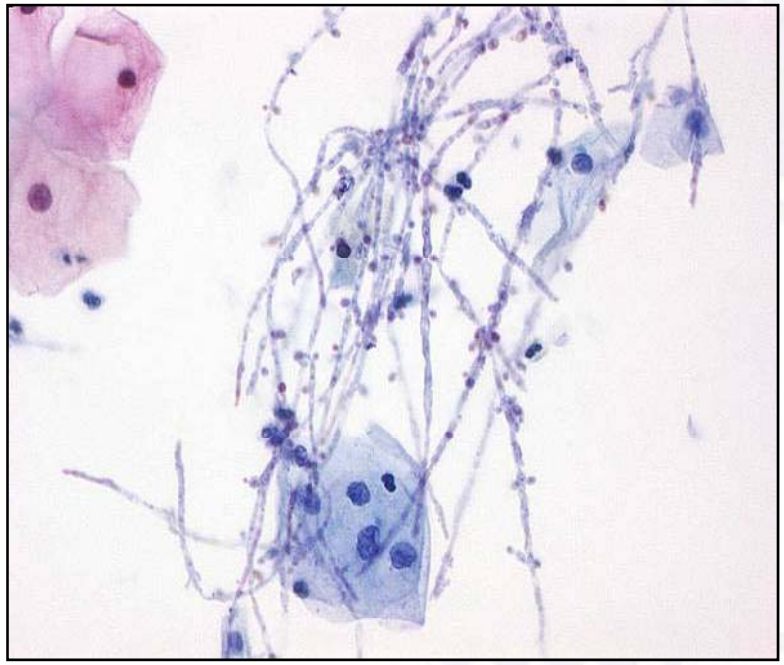

Candida albicans:
Fig. 21e: Tubular hyphae with segmentation, branching and budding.

Candida albicans:
Fig. 21f: Negative staining reaction.

Squamous metaplasia

p16^{INK4a} immunostain: <u>focal</u> distribution of positive cells in differentiating cell layers

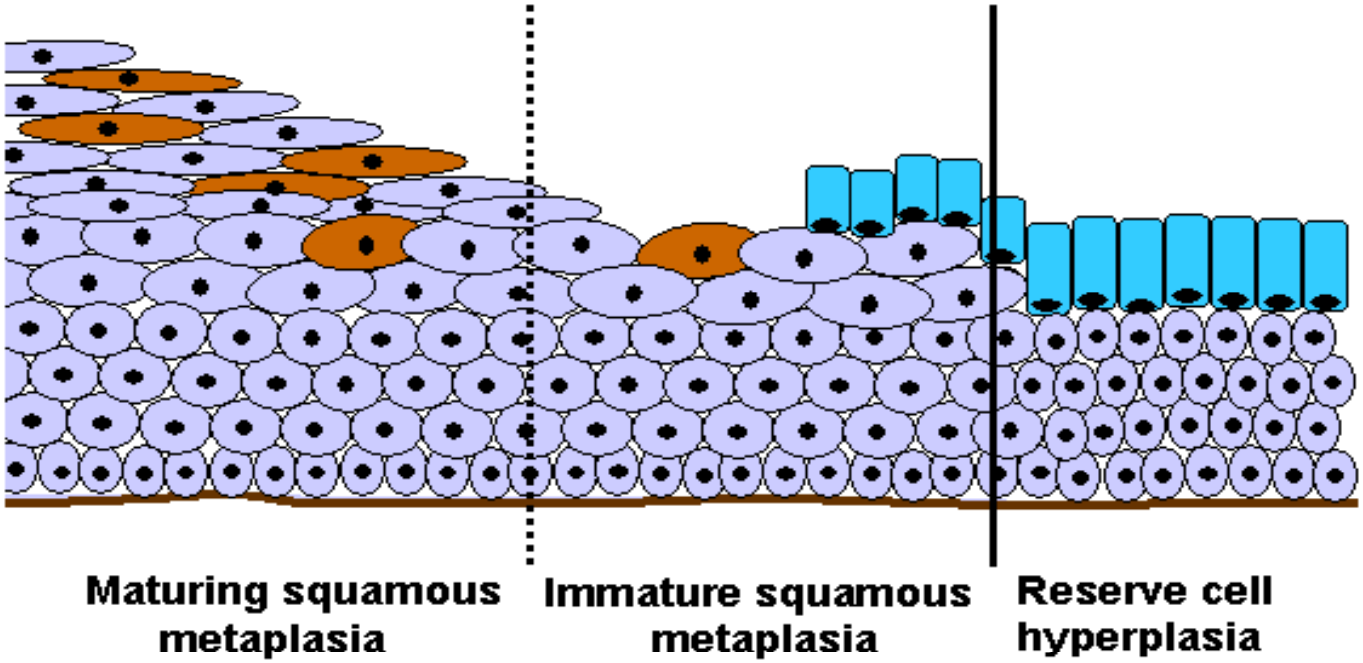

Fig. 22: Scheme of p16^{INK4a} immunostaining, transformation zone with squamous metaplasia / tissue repair

Metaplasic Changes I

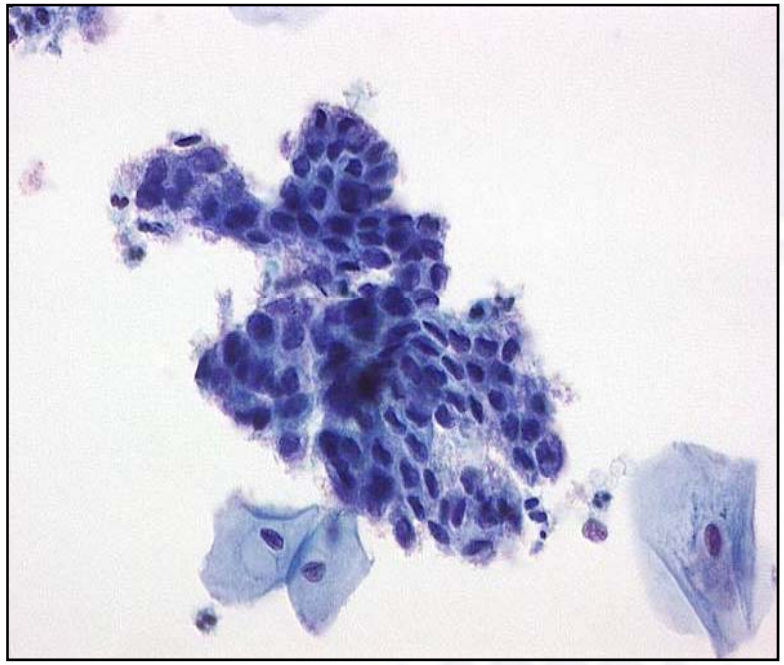

Cells from immature metaplasia and normal endocervical cells:
Fig. 23a: Group of columnar cells with small subcolumnar reserve cells. Relatively dense cytoplasm. Round to oval nuclei with finely granular chromatin. No nucleoli.

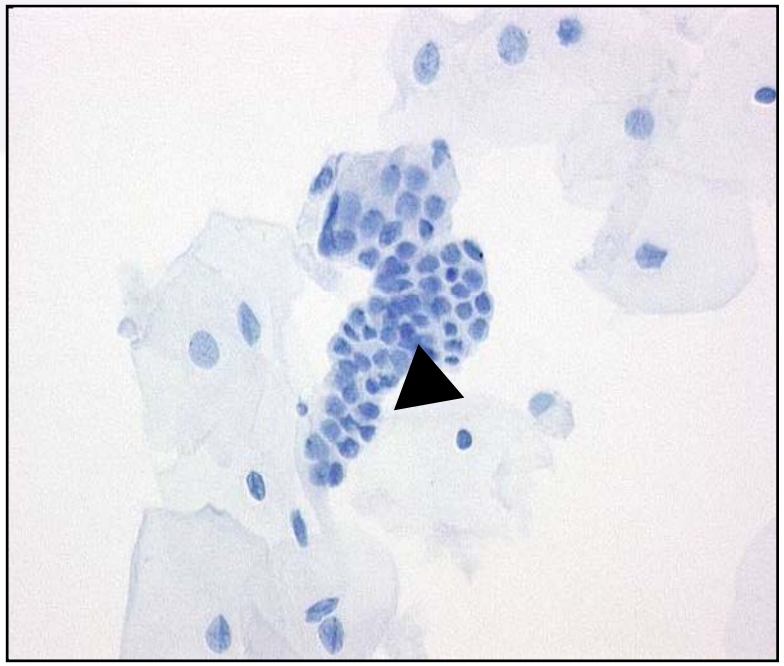

Cells from immature metaplasia and normal endocervical cells:
Fig. 23b: Subcolumnar reserve cells negative for p16INK4a.

Metaplasic Changes II

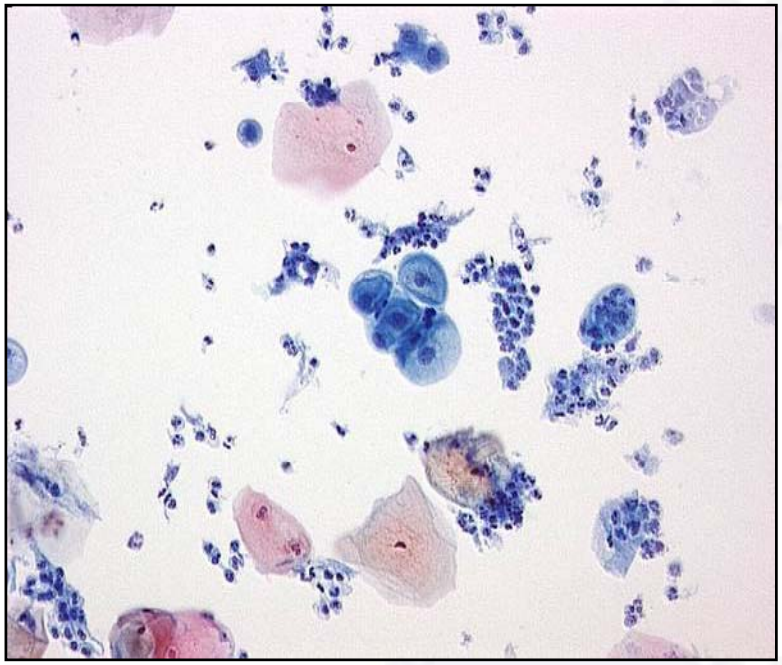

Maturing squamous cell metaplasia / tissue repair:
Fig. 24a: Polygonal cells of intermediate cell type with rounded corners. Uniformly finely granular chromatin.

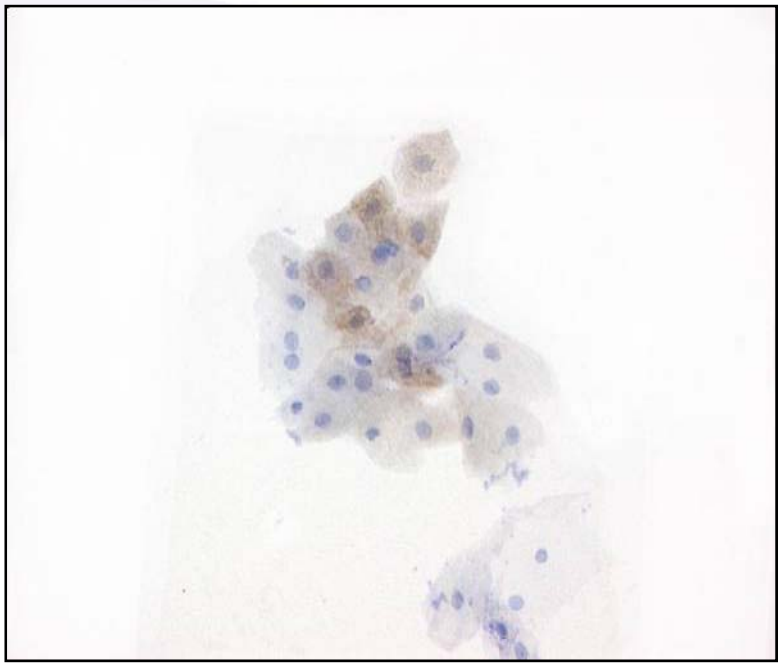

Maturing squamous cell metaplasia / tissue repair:
Fig. 24b: Group of relatively mature squamous epithelial cells shows positivity for p16INK4a in some cells, whereas others are negative.

Metaplasic Changes II

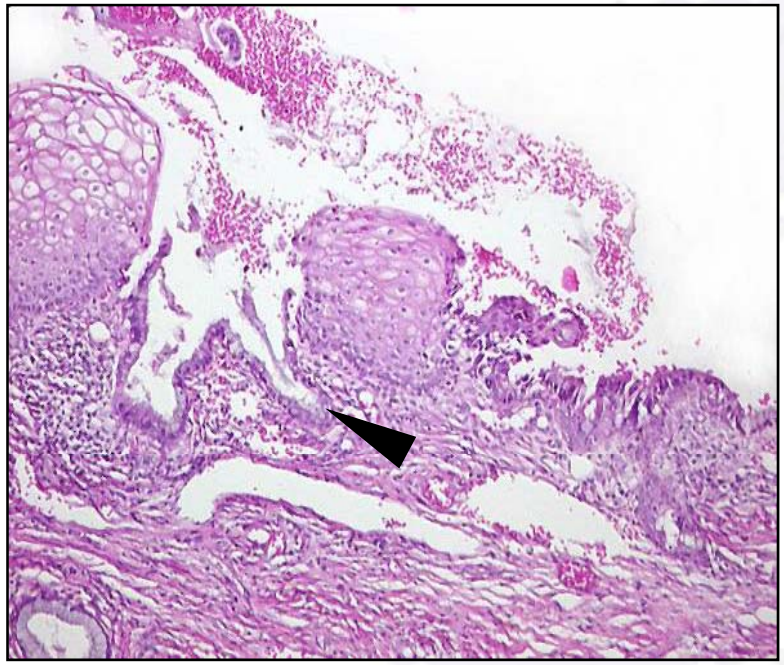

Transformation zone, maturing squamous cell metaplasia:
Fig. 24c: Regularly maturing squamous cells bordering to endocervical columnar cells (arrowhead).

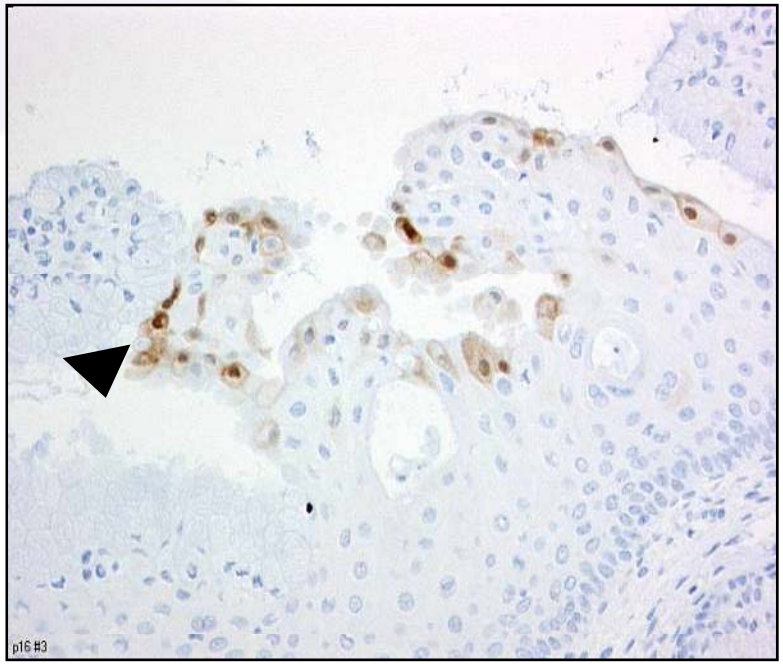

Transformation zone, maturing squamous cell metaplasia:
Fig. 24d: Some of the maturing squamous cells show cytoplasmic and nuclear positivity for $p16^{INK4a}$ in a sporadic distribution of the positive cells in superficial layers.

Tubal metaplasia

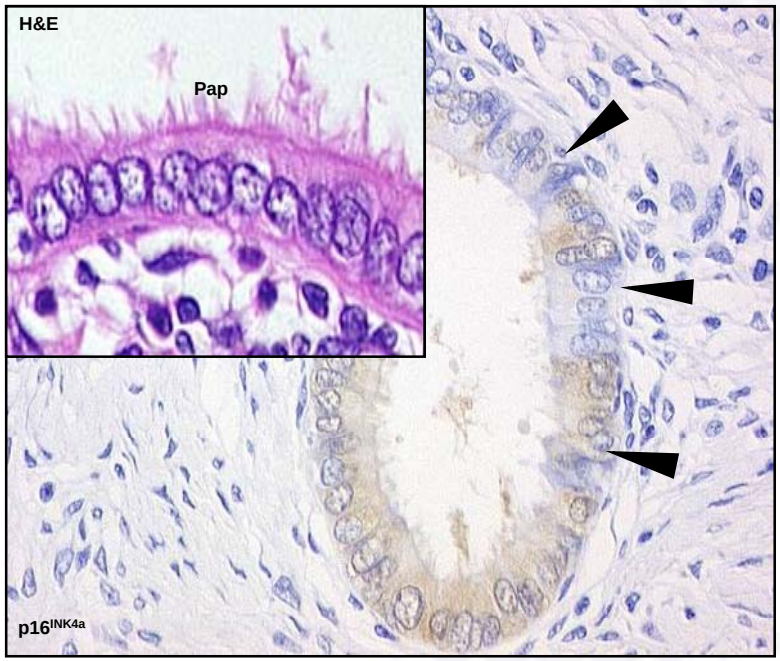

Tubal metaplasia
Fig. 25a: Ciliated columnar cells in a single cell layer lining an endocervical gland. Metaplastic cells show positivity for p16^{INK4a} only in part of the epithelial cells, neighboring cells are negative (arrowheads). Insert: Higher Magnification to demonstrate ciliated cells (H&E).

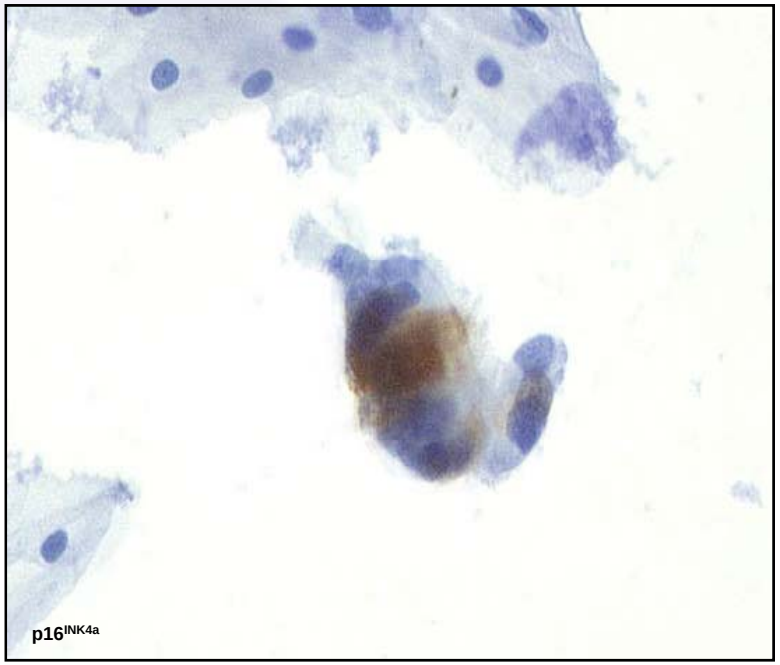

Fig. 25b: Small group of endocervical ciliated columnar cells. Chromatin somewhat coarser than in normal endocervical cells. No nucleoli.

Squamous Metaplasia

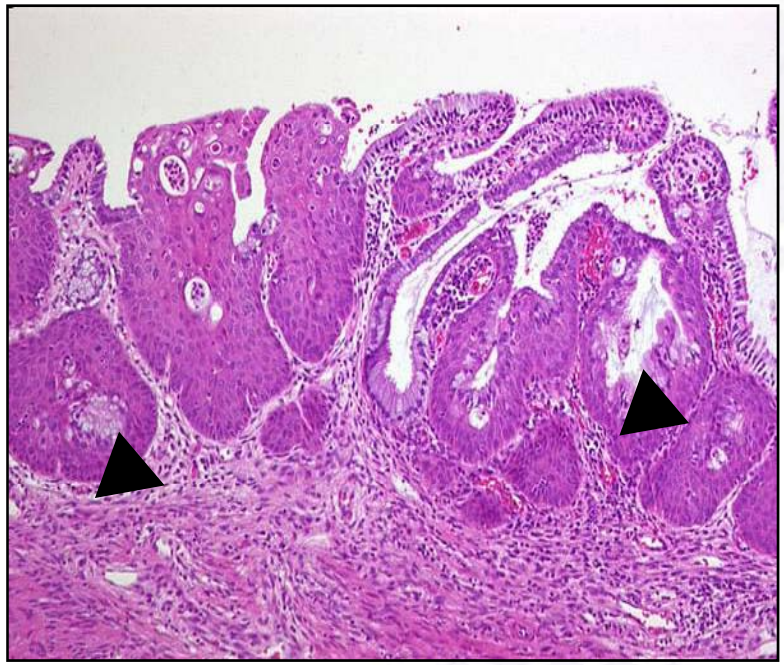

Immature squamous metaplasia:
Fig. 26a: Reserve cells, partly covered by a single layer of endocervical columnar cells (arrowheads) with focal differentiation to metaplastic squamous cells. Round to oval nuclei with finely granular chromatin.

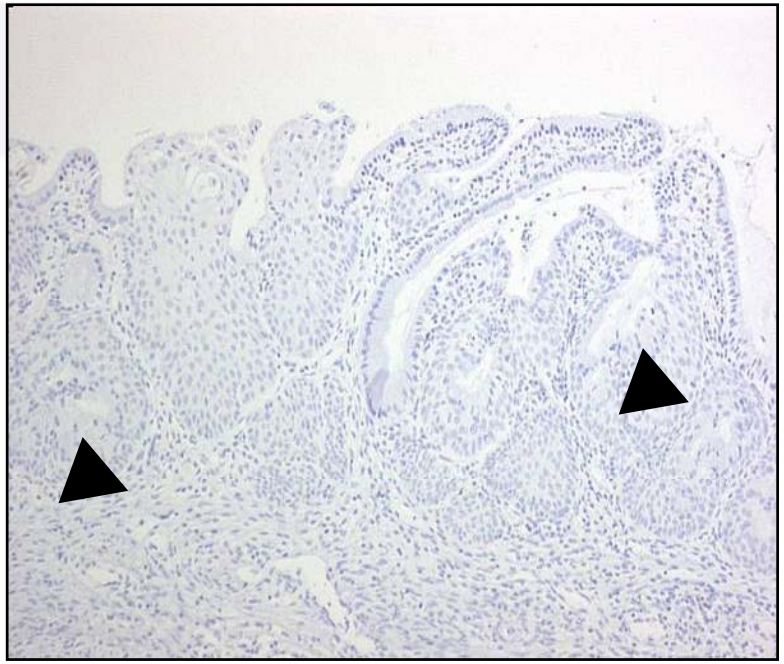

Immature squamous metaplasia:
Fig. 26b: No positivity for $p16^{INK4a}$ in subcolumnar reserve cells. Arrowhead: Endocervical columnar cells.